A litho-tectonic event stratigraphy from dynamic Late Devensian ice flow of the North Sea Lobe, Tunstall, east Yorkshire, UK

Jenna L. Sutherland[1, 2*], Bethan J. Davies[1], Jonathan R. Lee[3]

[1]Department of Geography, Royal Holloway University of London, Egham, Surrey, TW20 OEX, United Kingdom

[2]School of Geography, University of Leeds, Woodhouse Lane, Leeds, West Yorkshire, LS2 9JT, United Kingdom

[3]British Geological Survey, Keyworth, Nottingham, NG12 5GG, United Kingdom

*Correspondence to:
Jenna Sutherland
Email: gyjls@leeds.ac.uk
Tel.: 0113 343 3324

ABSTRACT

The central sector of the British-Irish Ice Sheet during the last glaciation was characterised by complex ice-flow reflecting interacting ice streams and changing dominance of different ice dispersal centres. At Tunstall, east Yorkshire, two subglacial till units have been traditionally identified as the Late Devensian Skipsea and Withernsea tills, and thought to record two separate ice advances onto the Holderness coast, from divergent ice flow directions. Our study presents the first quantitative lithological, sedimentological and structural evaluation of glacial sediments at the site. The lithological composition of both till units suggests that ice extended southwards from southern Scotland, incorporating material from north-east England and the western margin of the North Sea Basin. Notably, the bulk lithological properties of both the Skipsea and Withernsea tills are very similar. Subtle variations in colour, texture and lithology that do occur simply appear to reflect spatial and temporal variability in subglacial entrainment along the flow path of the North Sea Lobe. The relative arrangements of the units plus the fracture sets also indicates phases of intra-till thrust-stacking and unloading (F2), consolidation and shrinkage (F1, F3) suggestive of cycles of ice re-advance (thrusting) and ice-marginal retreat (unloading and shrinkage) possibly relating to active recession. The findings from this study reveal a sedimentary and structural complexity that is not recognised by the current Late Devensian till stratigraphy of east Yorkshire.

KEYWORDS

British–Irish Ice Sheet, North Sea Ice Lobe, Skipsea Till, Withernsea Till, Lithology, Provenance

1. INTRODUCTION

Palaeo-ice sheets are important analogues for understanding contemporary ice sheets, offering a record of ice sheet behaviour that can span millennia (Ely *et al*., 2019). The last British-Irish Ice Sheet (BIIS) provides an excellent analogue for understanding the character and behaviour of modern marine-based ice sheets due to its comparatively small size, accessible bed, and the wealth of pre-existing information (e.g. Evans *et al*., 2005; Livingstone *et al*., 2012; McMillan and Merritt, 2012; Clark *et al*., 2012; 2018). Approximately two thirds of the BIIS was marine-based, drained by ice streams and fringed by ice shelves in many places (Clark *et al*., 2012; Gandy *et al*., 2018, 2019), making it a good analogue for the West Antarctic Ice Sheet (WAIS; Hubbard *et al*., 2009). This is especially so because the BIIS deglaciated in response to rising temperatures and a rising sea level (driven by melting of other ice masses), which are the current forces that might cause collapse of the WAIS (Bamber *et al*., 2009; DeConto and Pollard, 2016). Reconstructing the behaviour of palaeo-ice sheets enables a better understanding of the long-term (centennial to millennial) behaviour of ice sheets within the Earth system. Only when the mechanisms from palaeo-ice sheets, such as the BIIS, are better constrained, can such knowledge be used for improving the next generation of numerical ice sheet models used in sea-level forecasting (Stokes *et al*., 2015; Ely *et al*., 2019).

The body of empirical evidence related to the BIIS has progressively developed over the last decade in particular (e.g. Clark *et al*., 2012, 2018; Hughes *et al*., 2016; Small *et al*., 2017;

Bateman *et al*., 2018; Bradwell *et al*., 2019; Davies *et al*., 2019; Ely *et al*., 2019; Lovell *et al*., 2019), producing an ever-expanding database of palaeo-ice sheet data, but there are still gaps in knowledge regarding ice-marginal processes (Roberts *et al*., 2013) and their implications for glacier dynamics. Eastern England and the North Sea Basin are the main areas of complexity and uncertainty due to multiple competing ice lobes and potential ice flow reversals (Evans *et al*., 2019). The ice limits, interactions between ice lobes, and their relative chronologies in this area are only broadly known and, without this understanding, the glaciodynamic history and the nature of the BIIS remains contested.

In order to address outstanding questions on the character and behaviour of part of the southeast sector of the last BIIS, this study has three main aims. Firstly, this study will determine the depositional processes and a relative event stratigraphy for the Late Devensian sediments observed at Tunstall, eastern England (**Figure 1**). Secondly, this study will determine the provenance of the glaciogenic sequence in order to reconstruct the glacial transport pathway for the deposits. Thirdly, this study will integrate this event stratigraphy and sediment provenance information into the broader Late Devensian evolution of the region and southeast sector of the last BIIS.

2. STUDY AREA AND PREVIOUS INVESTIGATIONS

A southward advance of the North Sea Lobe (NSL) of the last BIIS during the Late Devensian (Weichselian; Dimlington Stadial; MIS 2) resulted in the development of till sequences across parts of County Durham, east Yorkshire, Lincolnshire and north Norfolk (Pawley *et al*., 2006; Catt, 2007; Davies *et al*., 2009, 2013; Boston *et al*., 2010; Evans and Thomson, 2010; Bateman *et al*., 2011, 2015, 2017; Roberts *et al*., 2013). The glacial lithostratigraphy of the Holderness coast, east Yorkshire (**Figure 1B**), has traditionally been

subdivided into three till units (the Basement Till, Skipsea Till, and Withernsea Till respectively), based principally upon particle size distribution, sediment colour, clast lithology, heavy mineral composition and matrix calcium carbonate content (Madgett and Catt, 1978; Catt, 2007). Optically Stimulated Luminescence (OSL) ages constrain the timing of initial advance of the NSL into the region, and deposition of the Skipsea Till, to ~21.7 ka (**Figure 1**), reaching its maximum extent at ~19.5 ka (Evans *et al*., 2019) with offshore retreat occurring at ~18 ka (Bateman *et al*., 2011, 2015, 2017). The recession of the NSL was initially rapid followed by a series of near synchronous oscillations of the NSL, and subsequent deposition of the Withernsea Till at ~16.8 ka, before the final terminal retreat of the ice sheet occurring prior to ~15.5 ka (Bateman *et al*., 2017).

Catt (2007) described the Skipsea Till as possessing a dark-greyish brown (10YR 3/2) colour and occupying the whole Holderness area. The Skipsea Till is correlative with the Late Devensian Horden Till Formation in County Durham (Davies *et al*., 2009; 2012), based on stratigraphic relationships and sedimentary petrography. According to Pawley *et al*. (2008), on the basis of correlative luminescence dates, the north Norfolk equivalent of the Skipsea Till is the Holkham (Hunstanton) Till. However, recent OSL dating has suggested a slightly earlier incursion of ice into north Norfolk timed at ~21.5 ka (Evans *et al*., 2019). Bisat (1939) and Radge (1939), suggested that the Skipsea Till was deposited by ice flowing into Eastern England through the Stainmore Gap from the Lake District and Pennines, while the Withernsea Till originated from the Cheviots and Southern Uplands. Later studies documented a suite of erratics derived from Scotland, Northumberland, and the Cheviots (Catt and Penny, 1966; Madgett and Catt, 1978; Catt, 2007). Busfield *et al*. (2015) confirmed, from quantitative clast data and derived microfossils, that the Skipsea Till was sourced from southern Scotland, incorporating material from north eastern England, northeast Yorkshire and the western margin of the North Sea Basin.

The overlying Withernsea Till (dark-reddish brown, 5 YR 3/4 in its weathered form) by contrast is less widespread, cropping-out in south east Holderness **(Figure 1C**) (Evans and Thomson, 2010). North of Flamborough Head, the Withernsea Till reappears as the Upper Till Series of Edwards (1981, 1987), seen in coastal cliffs of Filey Bay. However, Bisat (1939) suggested that the till is confined to isolated basins within this area. The Withernsea Till can be less confidently provenanced to its source area although erratics recorded suggest a source from the Lake District and Pennines (Catt and Penny, 1966; Catt and Digby, 1988; Bell and Forster, 1991). The red colouration is also strongly suggestive of input of Permo-Triassic materials from the Sherwood Sandstone and/or Mercia Mudstone groups. The fragmented, crenulated ridges developed within the landscape of Holderness (**Figure 1C**; Evans *et al*., 2001; Evans and Thomson, 2010; Clark *et al*., 2018) and superimposed upon the Skipsea and Withernsea Tills have been interpreted as lateral moraines and also suggest an ice-flow direction from the north and east.

Using geochemical data from samples at seven sites along the Holderness coast, Boston *et al*. (2010) argued that the Basement, Skipsea and Withernsea Tills could not be statistically differentiated, with more variation within than between the tills. This raised significant questions regarding the stratigraphical correlation of Late Devensian tills in east Yorkshire and Lincolnshire. Boston *et al*. (2010) concluded that the till units are not lithologically distinct and that the current stratigraphy does not recognise the sedimentary and structural complexity produced by repeated onshore, possibly surging flow by a dynamic NSL along the eastern margin of the BIIS (based on stacked sequences; Evans and Thomson, 2010). Clast lithology has been used effectively to quantify ice-flow pathways and provenance for the Skipsea Till (Busfield *et al*., 2015), but no comparative work has yet been undertaken for the Withernsea Till.

With some of the most rapidly eroding coastline in northern Europe (Bird, 2010; Castedo *et al*., 2015), the Holderness coast provides an ideal opportunity to assess extensive cliff exposures through the Quaternary geology. Tunstall is centrally located within the limits of both the Skipsea and Withernsea tills (**Figure 1C**), offering a valuable opportunity for a comparative study between the two tills deposited in superposition. Excluding a comprehensive soil profile examination by Madgett and Catt (1978) (**Figure 1D**), there has been little previously published process or provenance work conducted at Tunstall. Due to this lack of quantitative and detailed analysis, the understanding of till genesis remains underdeveloped. The site at Tunstall, therefore, offers an excellent opportunity to use detailed clast lithological analysis and detailed process-based sedimentology to untangle the stratigraphic relationships, ice-flow pathways and provenance of the Skipsea and Withernsea Tills.

3. METHODS

We present new quantitative sedimentological investigations of the Late Devensian till sequence that crops-out above Cretaceous chalk bedrock at Tunstall, east Yorkshire (**Figure 1D**), together with a comprehensive clast lithological provenance analysis critical to the palaeoglaciological reconstruction of the eastern sector of the BIIS.

Eight exposures were logged in detail from 2 km of vertical coastal cliff sections at Tunstall, east Yorkshire (0°0'6.9"E, 53°45'24.7"N). At each site, vertical profile logs were compiled from cleared sections. Following procedures outlined in Evans and Benn (2004), the sedimentary characteristics were recorded including unit thickness, modal grain size, sedimentary and tectonic structures, degree of consolidation, matrix *vs* clast supported nature, grading and sorting of each unit, Munsell colour, bed geometry, and the nature of

contacts between the units. Sediments were described using standard facies codes (following Benn and Evans, 1998) and reclassified into lithofacies associations (LFAs) to aid regional correlation. In order to convey the lateral changes in architecture and localised complexity in structural features, detailed field sketches and cross sections, supported by photographic evidence, were utilised to accurately map the geometry of the exposures and create an overall facies architecture map.

A three-order clast morphological analysis was used, encompassing clast shape, angularity/roundness and stone orientation to help establish the depositional history of the sediment (cf. Evans and Benn, 2004; Hubbard and Glasser, 2005; Hambrey and Glasser, 2012). Where possible, palaeo-current measurements were taken on stratified deposits. Clast fabrics, striae measurements and eigenvector analyses followed Benn (1994) and Hubbard and Glasser (2005). The structural data is presented in equal area stereographic projections as poles to planes. Bulk samples for particle size analysis (PSA) and clast lithological analysis (CLA) were collected from a 2 m^2 area in each lithofacies to give a statistically significant, representative sample (Bridgland, 1986). The minimum sample size was 201 clasts; however, >300 clasts were counted in 4 of the 8 samples. At least two replicate samples from each lithofacies for both PSA and CLA were taken to ensure the heterogeneity within the stratigraphy was accounted for. Due to the spatial variability and clast-poor nature of the diamicton units, bulk samples of at least 10 kg were collected. PSA was undertaken in order to describe the textural properties of the sediments and support genetic interpretation (Gale and Hoare, 2012). PSA was conducted using a laser granulometer for particles <2000 μm and dry sieving for particles >2000 μm. The lithology of all recovered clasts in the 8-16 mm, 16-32 mm, and >32 mm size fractions was identified using a low-powered binocular microscope and compared to a reference collection and standard rock

identification criteria (Evans and Benn, 2004, Walden, 2004, Stow, 2005; Gale and Hoare, 2012).

Multivariate statistical analysis was performed on the clast lithological data using Principal Component Analysis (PCA). PCA is commonly used in both regional geochemical and lithostratigraphical studies (Gibbard, 1985; 1986; Cheshire, 1986; Scheib *et al*., 2011). The data are easily reduced into a smaller number of interrelated groups that reveal underlying patterns or 'principal components' within lithological datasets. PCA axes simplify and represent variation in the data (Davis, 1986) to identify key variables, and relationships between variables, within a dataset (Richards, 1998; Lee, 2003; Davies *et al*., 2009). The analysis was run using the covariance matrix method (Kovach, 1995) which is strongly affected by non-normally distributed data and outliers (Reimann *et al*., 2008). Like other exploratory multivariate statistical techniques, PCA provides eigenvectors, or 'principal component coefficients' to describe the relative significance of individual (lithological) components and their variability within the data set. Associated eigenvalues or 'principal component scores' record the percentage of the total variance of each principal component, in this case, measuring the importance of each lithology relative to each other in describing the characteristics of a particular sample.

4. RESULTS: SITE SEDIMENTOLOGY AND STRATIGRAPHY

4.1 Facies Architecture

The stratigraphic architecture of the exposures at Tunstall is summarised in **Figure 2**. Vertical profile logs 1 - 8 (**Figure 3a, b**) reveal four distinct Lithofacies Associations (LFAs). Bedrock is not exposed and the LFAs identified vary both vertically and laterally. The summarised relative stratigraphic succession observed in the field is as follows; dark

coloured diamict (LFA 1) exposed towards the north of the section, overlain by red-coloured diamict (LFA 2), which is in-turn overlain by clast-supported sands and gravels with a sharp, unconformable, undulating base (LFA 3). A distinctly white organic silt (LFA 4) crops-out intermittently for a short distance within the LFA 3 succession in the middle of the lateral section. Above LFA 4 is a thin unit of LFA 3b and the top of the sequence is capped by a thin soil horizon ~10 cm thick.

The surface of the cliff undulates, and the middle section has been heavily human-modified. The height of the section varies between 4 m at the lowest point, where there is a break in the cliffs for beach access, to ~12 m at the highest. Slumping along the length of the section is widespread due to the instability of the cliffs obscuring many of the *in-situ* sediments. An unusual feature of the section at Tunstall is the numerous natural cliff promontories that protrude out ~ 3m towards the sea. Coastal erosion is non-uniform and some spurs are more prominent than others. An even distance of 10 - 15 m separates the spurs from each other along the beach.

4.2 Lithofacies Descriptions

LFA 1

LFA 1 is a dark brown (7.5 YR 3/4), matrix-supported, massive and homogenised diamicton with a dense clay-matrix texture, containing clasts ranging from fine gravels to small boulders up to 25 cm in diameter (**Table 1**). It has an over-consolidated nature. The thickness of LFA 1 varies between 0 - 6 m and is exposed only in the northernmost part of the section (**Figure 2**; **Figure 3b**; Section logs 5 to 8). The majority of clasts within LFA 1 are sub-angular (34 %) to sub-rounded (38 %) (**Figure 6B**), incorporating a high proportion of facetted and striated clasts (**Figure 6E**). The overall clast morphology is dominated by 'blocky' shapes (**Figure 6C**). The diamicton contains numerous laterally-extensive thin (<5

cm) lenses of gravel that dip 30 ^{o} to the south and can be traced along the section in several places (**Figure 3b**; Section logs 7 and 8). It possesses a generally weak clast fabric at each locality sampled (**Figure 2**); with a polymodal distribution of points but clustering towards the southeast. Stringers also occur in the lower few metres of the unit, just above the beach level, persisting up to 1 m before pinching out. LFA 1 is fissile, observed particularly at the boundary between LFA 1 and LFA 2. The upper contact with LFA 2 is sharp with a concave base. The base of the LFA 1 was obscured by the beach.

LFA 2

LFA 2 is a massive, matrix-supported, bright reddish brown (5 YR 5/6) sandy diamicton (**Table 1**). LFA 2 is consistently exposed to the south of the section where the cliffs are ~11 m high (**Figure 2**). The average clast morphology of LFA 2 is 'blocky' (**Figure 6C**) with a high proportion of facetted (31%) and striated (6%) clasts (**Figure 6E**). Larger boulders and cobbles are observed at variable heights and orientations and are heavily striated with often more than one striae orientation (**Figure 2**). The clast fabric is weak, with a polymodal distribution of points but a fairly weak clustering from the northwest to the southeast (**Figure 2**). The striae measurements show a clearer directional indicator, towards the south-west, than the clast fabrics (**Figure 2**). The majority of clasts are sub-angular to rounded (**Figure 6B**). LFA 2 is largely massive at the macroscale, but stringers also occur as numerous streaks of red and black diamicton up to 10 cm thick (**Figure 4b**). Discontinuous lateral beds (~30 cm) of grey diamicton alternate between thicker units (>50 cm) of the brown diamicton (**Figure 4d, e**) with sharp contacts above and below the interbeds. Thin, dipping sand and gravel laminations towards the northeast are observed at variable heights within LFA 2. In Section log 5 (**Figure 3b**), cross-bedded gravelly sands were observed in LFA 2 and a gravel pod that pinches laterally. The gravel pod is composed of laminated fine sands and fine gravels that coarsen-upwards.

253 *LFA 3*

254 LFA 3 is best illustrated in Section Logs 1, 2, 4, 7, and 8 (**Figure 3a, b**). LFA 3 is laterally
255 variable, observed intermittently every few meters along the length of the exposure, often
256 capping the sequence just below the soil horizon. Overall, there are three lithofacies present
257 within LFA 3; planar laminated dark clays and silts (LF 3a), planar, cross-bedded fine sands
258 (LF 3b), and cobbles and gravels (LF 3c). The basal contact of LFA 3 is undulating, with
259 elevations ranging from 1.2 m to 8 m. It is repeatedly down-cut into the underlying
260 diamicton (LFA 1 or 2) in a concave-shaped depression and has a sharp, erosive base (e.g.
261 **Figure 3a**; Section log 1). The upper contact with either LFA 4 or the soil horizon is planar
262 and sharp.

263 LF 3a is dominated by horizontal laminated dark clays and silts, which coarsen upwards into
264 massive fine sands (LF 3b). Thin (<5 cm) laterally-continuous seams of coal fragments and
265 particles (mm – cm) occur within the sandy unit of LF 3b. LF 3c consists of well-sorted,
266 well-rounded, clast-supported coarse pebbles and cobbles (**Table 1**) that are stratified and
267 imbricated towards the northwest (**Figure 3a;** Section Log 4**; Figure 4g, h**). Randomly
268 orientated, clast-supported, coarse gravels of LF 3c typically infill the concave structures
269 (**Figure 4g**) and numerous pebble lags are observed along the bases of the channel-like
270 structures. The majority of clasts are well-rounded (28 %), rounded (32 %) and sub-rounded
271 (24 %), with only 4 % faceted and no clasts striated (**Figure 6B**, **C**, **E**). Up to 14 % of the
272 stones are broken. The unit thickness of LF 3c is typically thicker than LF 3a and b.

273 *LFA 4*

274 LFA 4 is laterally discontinuous and only crops-out within LFA 3 near the surface of the
275 southernmost part of the section (**Figure 4f**). LFA 4 comprises a bright white (7.5YR 8/1)
276 silt which highly calcareous (57 % calcium carbonate content). The contacts above and

below LFA 4 are very sharp and linear. The unit of the lower boundary has a slight elliptical shape covering a discontinuous lateral extent of roughly 300 m. The deposit is uniformly 20 cm thick and is densely packed with small shells deposited in their life position. The majority of the shells within the sediment are freshwater gastropods including abundant *Radix bulthica*, *Lymnaea peregra*, and *Galba truncatula*, but other freshwater snails *Planorbis viviparis*, *Valvata crisata* and aquatic bivalves of *Pisidium* genus are also present.

4.3 Lithofacies interpretations

LFA 1 and 2

LFA 1 and LFA 2 possess many bulk characteristics of a subglacial traction till such as their matrix-supported texture, highly fissile, and over-consolidated nature, in addition to the presence of faceted and striated lithologies of wide-ranging provenance (cf. Evans *et al*., 2006). A subglacial traction till is defined by Evans *et al*. (2006) to include sediments that accreted by sliding over and/or deforming at the glacier bed, sediment released directly from the ice by pressure melting, and sediment completely or largely homogenised by shearing. The fissile structures, observed at the boundary between the tills are interpreted here to be very small, thin thrust faults. Clast rotation within subglacial traction tills results in shape alignment of elongate, low-sphericity grains such as those observed in LFA 1 and 2 (**Figure 6B, C**). Where clasts have been brought into contact while lodged on a rigid bed and moving in the subglacial traction zone, they typically have bullet-shaped and faceted ends (Boulton and Hindmarsh, 1987; Kruger, 1979, 1984, 1994; Sharp, 1982), such as those in LFA 1 and 2 (**Figure 6E**). Other structures within both lithofacies indicative of lodgement, such as their massive homogenised appearance, occur in association with structures indicative of subglacial deformation, including stringer initiation and deformed inclusions of LFA 1 in LFA 2 (**Figure 4b**, **d**, **e**), as well as weak clast macrofabrics (**Figure 2; Figure 3a, b**); Evans *et al*., 1995; Hicock and Fuller, 1995, Hart 1997; Bennett *et al*., 1999; Roberts and

Hart, 2005). Stringers of red and black diamicton (particularly in LFA 2) are, therefore, interpreted as tectonic laminae produced by the progressive shearing and attenuation of soft sediment inclusions (Hart and Roberts, 1994; Phillips *et al*., 2008). Most of these structures indicate that the till was formed under low strain conditions with elevated porewater pressures (van der Wateren, 1995; Hiemstra *et al*., 2007; Lee and Phillips, 2008); however, strain rates can vary both spatially and temporally as pore-water pressure fluctuates, creating a mosaic of deformation (Piotrowski *et al*., 2004; Lee and Phillips, 2008; Lee, 2009). This may explain why some of the sections at Tunstall, particularly of LFA 1, are more massive and are completely homogenised than others, while delicate deformation structures, such as stringers, are preserved elsewhere.

LFA 3

Overall, a glaciofluvial origin is suggested for LFA 3 based upon the coarse-grained characteristics of LF 3c in addition to the evidence for abrupt discharge fluctuations, recorded in discontinuous, lensate bodies of cross-bedded sands (LF 3b) which are likely to be post-glacial winnowed lags. These packages of massive to crudely horizontally-bedded sheets, separated by lower discharge scour infills, are typical of strongly episodic fluvial sedimentation, classified as gravel sheets by Miall (1977) and Maizels (1993). The horizontally-bedded glaciofluvial outwash assemblage records rapidly fluctuating discharges, as evidenced by abrupt vertical changes from boulder gravels to the laminated sediments typical of overbank fines or waning discharge drapes (Miall, 1977, 1985; Collinson, 1996).

The irregular, concave base of the LFA 3 basal contact is interpreted as an erosional base with concave-up bases and flat tops (**Figure 4g**) permitting isolated channelized forms that have been shaped by the erosive force of water incising into the underlying sediments. The gravel facies that infill the isolated channel forms, in addition to the strong variation in

height of these channels, support the interpretation of deposition in a proximal setting for LFA 3, interpreted as the product of high energy proglacial outwash when the ice was retreating (Miall, 1977; Maizels, 1995). Due to the lack of large-scale trough cross-bedding and the cyclic fining-upwards sequence of gravels, sands and silts, distal proglacial outwash sedimentation has been excluded as a mechanism for the deposition of LFA 3. Instead, LF 3a could have been deposited by under-melt at the ice-bed interface in subglacial canals (cf. Walder and Fowler, 1994), perhaps indicative of ice-bed decoupling and sliding, or in Nye channels, similar to those that have been observed elsewhere in Devensian sediments in Northeast England (Eyles *et al*., 1982; Davies *et al*., 2009). The pebble lags evident in LFA 3a point to evidence of bedload saltation, whereby pebbles have been rolled along in flowing water at the boundary of the bed and formed a lag.

The direction of the imbricated clasts of LF 3c indicates a palaeo-flow direction from the northeast. The majority of clasts in LFA 3c are rounded (**Figure 4b; Figure 6B**) which indicates highly abrasive high energy conditions in a fast-flowing current, whereas the lenses of bedded sands, and stratified gravels are indicative of moderate flow regimes with frequent changes in flow regime and sediment supply. An increasing energy regime is also implied by the upwards coarsening of the sequence. Changes in the dominance of flow suggest the presence of fast, hyperconcentrated flows, as well as slower moving, lower energy flows.

LFA 4

The freshwater gastropods *Radix bulthica*, *Radix peregra*, *Galba truncatula*, *Panorbis viviparous* and *Valvata cristata* all inhabit the same type of environment; stagnant or slow moving water (Kerney *et al*., 1980). Due to the abundance of these freshwater gastropods, the depositional environment is inferred to be a spring-fed vegetated calcareous pool or shallow film of water trickling across wet ground such as a Tufa (Garnett *et al*., 2004). Tufa

is a variety of limestone formed by the precipitation of carbonate minerals from ambient temperature water bodies and forms either in fluvial channels or lacustrine settings. The deposit at Tunstall is likely to have occurred from an emergence of a spring or seep, due to its thin bed thickness and discontinuous lateral extent. Spring-fed paludal deposits are widespread on or near limestone bedrock (Andrews *et al*., 2000).

4.4 Structural genesis

Fracture description

A series of horizontal and vertical fractures dissect the lower sections of the cliffs at Tunstall. In places, these fractures have been eroded and enlarged by wave action. Overall, four distinct fracture sets are observed within the cliff exposures; three sub-vertical sets (F1, F3 and F4), punctuated by a sub-horizontal fracture set (F2). Given their continuous presence and abundance along the cliff exposure, the fractures are inherent structural features of the deposits at Tunstall.

The F1 fracture set occurs discontinuously at the base of the cliffs within LFA 1 material. They are vertical to sub-vertical fractures, up to 1.5 m in length, that strike broadly northeast-southwest and variably dip towards the northwest and southeast at angles >75 ˚ (**Figure 5**). The density of the fractures is spatially variable, being more densely concentrated at the base of each cliff promontory but occurring along the entire length of the described section (**Figure 4a**, **c**, **d, i**). The density of fractures varies with zones of high density (spacing ranging from 1 - 20 cm) and low density (spacing range from 20 - 100 cm) fracturing. The F1 fracture set extends up to, and is truncated by, a large persistent horizontal fracture (F2).

Horizontal fracture, F2, forms a laterally-persistent horizon, truncating F1 and separating beds of lower and upper unit of LFA 1 (**Figure 4c, i**). F2 can be traced discontinuously

along the cliff sections typically up to 2 m above the level of the foreshore. Dip and dip azimuth measurements collected on the fracture surfaces demonstrate a spread polymodal distribution with shallow (<14 ˚) dips (**Figure 5**) indicating a gently undulating sub-horizontal fracture plane.

The F3 fracture set extend upwards from the sub-horizontal fracture F2 occurring within the upper unit of LFA 1 and also in LFA 2, but are cross-cut in-turn by LFA 3 and 4. This demonstrates, that F3 post-date F2 but pre-date the deposition of LFA 3 and 4. They are visible discontinuously along the length of the section, and are sub-vertically inclined (>78˚) and have a marked straightness and parallelism (**Figure 5**). They range in length from 10 cm to 4 m and strike broadly east northeast - west southwest.

Fractures F4 occur only within the cliff promontories where they truncate the entire vertical section (including F1-F3) with their bases occurring beneath beach level. The fractures are slightly curved fractures that radiate upwards, sub-parallel to the margins of the promontories. The fractures widen upwards (up to 2 m) and towards the promontory margins.

Fracture Interpretation

Fractures F1-F3 are interpreted as extensional fractures (mode 1 fractures) due to the lack of evidence for slip or displacement along the joints. Collectively they are interpreted to form broadly perpendicular sets of sub-vertical (F1 and F3) and horizontal (F2) joints formed by glacier unloading, consolidation and drying of the diamicton. Sub-horizontal joints (F2) are unloading joints (also called release joints) formed as the applied vertical load (ice overburden) was removed. The removal of the overburden caused the vertical compressive stress to be released resulting in fracturing being initiated probably along a pre-existing plane of weakness. The continuous nature of F2 implies that this pre-existing plane of

400 weakness was laterally extensive, for example a shear plane, which bounded two beds of
401 LFA 1.

402 The origin of vertically-aligned fractures (F1 and F3) is also interpreted to be an artefact of
403 unloading but also subsequent drainage, drying (Boulton and Paul, 1976) and shrinkage of
404 the sediment (Mertens *et al*., 2003). Within this scenario, removal of the ice overburden led
405 to a reduction in the differential stress and a switch from dominant vertical to horizontal
406 compression (Maltman, 1994). Subsequent reduction in the horizontal compression and a
407 switch to tensile stresses would have promoted shrinkage which in-turn would require a
408 moderate differential stress to be maintained to prevent shearing (Mertens *et al*., 2003;
409 Dehandschuttter *et al*., 2005).

410 F4 fractures are focussed around the coastal spurs or promontories and cross-cut all other
411 parts of the sequence demonstrating that these are the last features to have formed. Their
412 geometry, sub-parallel alignment to the margins of the promontories and the upwards-
413 widening of the fractures, suggests that they formed by the lateral release of an applied load
414 (i.e. the removal of cliff material by coastal erosion; Cossart *et al*., 2008; Genter *et al*.,
415 2004).

416

417 ## 5. RESULTS: CLAST PROVENANCE

418 ### *5.1 Clast lithological analysis*

419 Clast lithological data (**Table 2)** shows average percentages for each LFA. Eight samples
420 were analysed in total, four from LFA 1, three from LFA 2, and one sample from LFA 3.
421 **Figure 7** shows the results of clast lithological analysis for each sample. Representative
422 photographs are shown in **Figure 8**. The dominant lithologies within LFA 1 are
423 Carboniferous Sandstone (13.6 %), Jurassic Mudstone (11. 7 %), Cretaceous chalk (10.4 %),

Carboniferous Limestone (9.5 %), Magnesian Limestone (6.6 %), and Jurassic Sandstone (6.2 %), (**Figure 7**). Other clast lithologies within LFA 1 include Mercia Mudstone (3.02 %), Old Red Sandstone (2.9 %), Sherwood Sandstone (2.7 %), and coal (2.1 %). There are relatively low amounts of Whin Sill dolerite (1.9 %), greywacke (1.2 %), diorite (0.8 %), Jurassic limestone (0.6 %), andesite (0.6 %), and rhyolite (0.5 %). Notably, there is a lack of distinctive Lake District granites and erratics.

LFA 2 contains higher percentages of Carboniferous sandstone (18.4 %), undistinguished arkosic sandstone (4.6 %), Whin Sill Dolerite (4.3 %) and Sherwood Sandstone (3.1 %), than LFA 1, but lower amounts of Carboniferous limestone (7.4 %), Jurassic mudstone (7.0 %) and Cretaceous chalk (6.6 %). There are slightly higher percentages of igneous lithologies present within LFA 2, such as micro-granite (1.1 %), rhyolite (1.1 %), andesite (1.0 %), basaltic porphyry (1.0 %), rhyolitic porphyry (0.6 %), andesitic porphyry (0.8 %) and gabbro (0.3 %).

LFA 3 is dominated by a high proportion of Carboniferous sandstone (26.5 %) (**Figure 7**). Other lithologies present in significant amounts are Jurassic mudstone (6.5 %), Old Red Sandstone (6.2 %), yellow sandstone (5.4 %), red siltstone (5.0 %), and Jurassic sandstone (3.1 %), plus an elevated amount of Whin Sill dolerite (9.6 %), much higher than is present in either LFA 1 (1.9 %) or LFA 2 (4.3 %).

5.2 Clast durability

The two till units at Tunstall contain striated, faceted, far-travelled, non-durable erratics as well as a matrix-supported sediment, indicating that a diverse suite of bedrock (including softer lithologies of chalk and coal) have been eroded subglacially, cannibalised and incorporated into the sediment. This suggests that the genesis of both tills was largely the result of comminution and soft-sediment mixing (Roberts *et al.*, 2013). The mixed

448 lithological assemblages within LFA 1 and 2 suggest subglacial cannibalism from a number
449 of different regions. CLA confirms that both tills have not been deposited close to their
450 sediment provenance areas since their lithological composition is heterogenous, indicating
451 an increasing number of sources rocks over which the glacier has travelled (cf. Boulton,
452 1996a, b). It is unlikely that the abundance of soft, non-durable, sedimentary lithologies
453 (**Figure 9)** including Jurassic, Permian and Carboniferous limestone, Jurassic mudstone,
454 coal and chalk would have survived multiple episodes of re-working, particularly within a
455 highly abrasive, subglacial environment (cf. Lee *et al*., 2002).

456 LFA 3 contains a diverse suite of erratics similar to those in LFA 1 and LFA 2 but there is a
457 noticeable paucity of non-durable lithologies such as Cretaceous chalk, Permian Magnesian
458 Limestone, and Jurassic Mudstone (**Figure 9**). The major lithological difference between
459 LFA 3 and LFA 1 and 2 is the marked increase in Whin Sill dolerite (~10 %) in LFA 3,
460 compared with <5 % in both LFA 1 and LFA 2. Almost the entire lithological content of
461 LFA 3 consists of far-travelled, durable lithologies (**Figure 9**). The presence of durable
462 lithologies support the interpretation of a high-energy environment as softer, non-durable
463 sedimentary lithologies are likely to have been destroyed by abrasion and attrition. The coal
464 fragments observed in LF 3b are an anomaly since coal is a low-durability material.
465 However, the relative buoyancy of coal aids its preservation during high-energy transport
466 whilst its deposition implies a rapid reduction (still-water) in energy regime (cf. Lee *et al*.,
467 2015).

468 *5.3 Principal Component Analysis (PCA)*

469 PCA was undertaken on the clast lithologies in an attempt to identify lithological similarities
470 between samples and determine the significant lithological variables and their
471 interrelationship. In total eight different principal components (PC 1 – 8) collectively
472 account for the lithological variability within the dataset. Three principal components (PC 1

– 3) account for 99.2 % of the total variability within the dataset. PC 1 explains 94.3 % of the sample variation, whilst PC 2 accounts for 3.6 %, and 1.3 % is accounted for by PC 3. **Figure 10a, b, c** shows the differences between lithofacies samples in relation to the principal component scores (PC 1 – 3). Samples with similar clast compositions are expected to cluster close together. PC 1 does not discriminate between the till samples (LFA 1 and 2) and the clast lithofacies (LF 3c) (**Figure 10a**). The samples do not cluster into distinct groups, and the variation between samples in each LFA is large, indicating a broad clast lithological spread throughout the samples. LFA 3 plots individually (**Figure 10a, c**), due to the fact it has fewer non-durable lithologies (**Figure 9**). All other samples show stronger variations along the axis of PC 1.

Based upon PC 1 there appear to be no major discernible differences in till lithology evident between LFA 1 and LFA 2. However, there are subtle variations (inverse relationships) between the other principal components (PC 2 and PC 3; **Figure 10b** and **c).** The principal component scores suggest the correlation of samples with the established regional lithostratigraphy (Skipsea and Withernsea Till) cannot be defined by bulk lithology (e.g. PC 1) mirroring results from other geochemical data analyses (Boston *et al*., 2010). The inability of the method to discriminate between the two tills could be a consequence of the small sample number taken from each of the lithofacies as this can create an artificially high skew. Additionally, the stratigraphic position of LFA 2 cropping-out above LFA 1 is also likely to affect its lithological composition, since the bedrock would have already been mantled with till, and a re-advance would at least locally cannibalise the underlying till. The lithology of LFA 2 differs slightly, as shown by the more durable clast content (**Figure 9)**. PC 2 however, is able to discriminate between LFA 3 and the other till samples.

The principal component coefficients also identify key relationships between the main source provinces for the clast lithologies (**Figure 10d, e, f**). PC 1 highlights the abundance

498 of Carboniferous and Jurassic material relative to other clast lithologies, accounting for 94.3
499 % of the lithological variability within the samples. PC 2 (3.6 %) shows an inverse
500 relationship between Carboniferous, Old Red Sandstone (positive), and Jurassic, Permian,
501 and Cretaceous lithologies (strongly negative). PC 3 (1.3 %) demonstrates an inverse
502 relationship between Carboniferous and Triassic lithologies (strongly positive) and Whin
503 Sill dolerite and Old Red Sandstone (strongly negative). Collectively, the principal
504 component coefficients demonstrate complex shifts in clast lithological variability
505 throughout the Tunstall sequence. Different processes relate to the suite of clasts present in
506 each LFA, particularly between the tills (LFA 1 and 2) and glaciofluvially transported
507 material (LFA 3). Whilst clast preservation during transportation is likely to play a
508 significant role, it is likely that the relationships observed reflect considerable temporal and
509 spatial variability (including intra-till) in the entrainment of materials from the subglacial
510 bed along the ice flow path. This may reflect a temporal and spatial partitioning within the
511 subglacial bed, both in terms of areas of bedrock cover and zones of subglacial erosion, with
512 areas of the subglacial bed either buried by younger superficial deposits or strain rates being
513 too low to drive erosion. A zonal approach to glacial erosion likely relates to the suite of
514 clasts found within the tills, whereas the lack of local lithologies within LFA 3 is likely a
515 result of high energy transport.

516 *5.4 Till provenance*

517 In both till units, LFA 1 and LFA 2, Carboniferous and Jurassic components constitute >50
518 % of the lithological composition of the samples (**Figure 7**). There has been an abundant
519 incorporation of Carboniferous sandstone, limestone and coal, which are characteristic of
520 the bedrock strata from North Yorkshire, County Durham and Northumberland (Taylor and
521 Eastwood, 1971; Jones *et al*., 1995). Far-travelled sedimentary lithologies include the
522 Magnesian limestone (Cadeby Formation), which crops out extensively across north

523 Yorkshire, southern County Durham and offshore (Smith, 1995). Jurassic components are
524 traced back to outcrops in the regional area of the Cleveland basin and Redcar mudstone
525 formations in the Tees Bay (Macklin, 1998) and around Middlesbrough (Kent, 1980). Albeit
526 in low abundance in the tills, oolitic limestone is also typical of the Jurassic strata in the
527 northern part of the Cleveland basin. The Permo-Triassic Sherwood Sandstone Group
528 outcrops from the Tees Estuary to the Vale of York and the Midland Valley of Scotland
529 (Cameron and Stephenson, 1985).

530 Rare, far-travelled erratics in LFA 1 and LFA 2 include Lower Palaeozoic greywacke
531 (**Figure 8a**), which is likely to have been derived from the Southern Uplands (Greig and
532 Pringle, 1971). Devonian Old Red Sandstone clasts (**Figure 8c**) are likely to have a
533 provenance from the Midland Valley of Scotland (Trewin, 2002). Crystalline, metamorphic
534 lithologies such as schist, gneiss, diorite and k-feldspar rich granites and granodiorites
535 characteristic of the Scottish Grampian Highlands are present (**Figure 8g**, **j, k**), but in
536 extremely low abundance. This might suggest that these clasts have been re-worked from
537 the widespread Old Red Sandstone conglomerates that contain Dalradian material in the
538 Midland Valley (Cameron and Stephenson, 1985) or that their proportions have been diluted
539 by the incorporation of more local materials. K-feldspar granite clasts could also be derived
540 from the Cheviot Hills. Both tills contain purple to reddish-brown rhyolites, greenish-brown
541 andesites and porphyries (**Figure 8d**, **h**), which are characteristic of the Devonian Cheviot
542 Volcanic Formation that straddles the border between Northumberland and Scotland
543 (Toghill, 2011; Robson 1976). Rhyolite and andesite can also be attributed to the Lake
544 District, but the reddish-pink nature of the majority of rhyolites from Tunstall (e.g. **Figure**
545 **8h**) indicate a stronger presence of feldspar, characteristic of outcrops in the Cheviot Hills
546 (Robson, 1976). The Cheviot Hills is, therefore, established as the principal source region

for many of the igneous lithologies due to the large extent of felsic intrusive material in this area.

The overall lithological composition of both tills (LFA 1 and LFA 2) suggest that they were deposited by ice that flowed southwards down the present east coast of England. Source regions for the ice, indicated by the clast lithological composition, include the Midland Valley of Scotland, Southern Uplands and East Grampian Highlands, before ice entrained erratics from the Cheviots, Northumberland and Durham (**Figure 11**) moving southwards to the Holderness area.

6. DISCUSSION

6.1 Implications for the Devensian Stratigraphy of eastern England

LFA 1 and 2 are both massive, matrix-supported diamictons. At the macroscale, both units appear to possess a similar texture, particle size distribution and clast content. A chi-square test on the particle size distribution (**Table 1**) demonstrate that both tills cannot be differentiated on the basis of particle size ($\chi^2_{calc}(0.002) < \chi^2_{crit}(0.35)$), meaning that they could originate from the same source material. Other similarities between LFA 1 and 2 include laminations of gravel that are observed sporadically within both units and stringers that also occur at the base of both LFA 1 and 2. However, there are also subtle meso-scale (cm to m) variations between LFA 1 and 2 and distinguishing characteristics are matrix colour and fracture density. Along the length of the section there is only one short exposure where the lower two LFAs can be observed in superposition (**Figure 3b;** section log 5; **Figure 4i**). At this boundary, the contact between the units is sharp and highly fissile. There are also sand and gravel interbeds at the contact. The colour contrast at this boundary between LFA 1 and 2 is sharp. LFA 1 is darker in colour, particularly at the base, due to

being constantly saturated with water from the sea at high tide. Fissile structures are more abundant within LFA 1 than LFA 2, particularly at the contact where the upper contact with LFA 2 is sharp with a concave base. LFA 1 is slightly more stone-rich and more heavily fractured at the base than LFA 2 (**Figure 4i**).

Previous interpretations of the stratigraphic sequences along the Holderness coast have suggested that two Late Devensian tills are present - the Skipsea and Withernsea tills (Catt and Penny, 1966; Madgett and Catt, 1978; Bell and Forster, 1991; Bowen, 1999; Bell, 2002; Catt, 2007). These classifications are founded largely on the basis of changes in matrix colour and clast lithological assemblage (Catt and Penny, 1966; Madgett and Catt, 1978; Bowen, 1999; Catt, 2007). In this study, LFA 1 is interpreted as a subglacial traction till equivalent to the Skipsea Till on the basis of its dark brown colour, greater chalk content, and northern clast erratic assemblage. This interpretation is regionally supported by other investigations of tills which correlate stratigraphically to the Skipsea Till, such as the Horden Till Formation at Whitburn Bay (Davies *et al*., 2009), other areas of east Yorkshire (Catt, 2007; Boston *et al*., 2010; Evans and Thomson, 2010), Northumbria (Eyles *et al*., 1982), and offshore (Carr *et al*., 2006; Davies *et al*., 2011). Based on its stratigraphic position (overlying the Skipsea Till), LFA 2 should therefore be assigned to the Withernsea Till. Sedimentologically, LFA 2 is similar to previous descriptions of the Withernsea Till; it is a dark reddish brown sandy diamicton. However, the lithological data presented in this study does not support the concept of LFA 2 being an entirely different till, as its bulk lithology is indistinctive from the Skipsea Till.

The till sequences that crop-out along the east coast of England have consistently been referred to as the product of either Scottish or east coast ice from the North Sea ice lobe (NSL), or Stainmore ice. Clast lithological data from this study concludes that the tills possess similar lithological characteristics and provenance. Evidence of Lake District input

(cf. Bisat, 1939; Radge, 1939; Catt and Penny, 1966; Catt and Digby, 1988; Bell and Forster, 1991) was not replicated in this study and the lithological analysis at Tunstall reveals no indicator erratics from the western part of England, now widely discredited nevertheless (Davies *et al*., 2019). This confirms that the tills are not associated with the same ice lobe as the Vale of York glacier that formed the York and Escrick moraines (Phillips, 1827; Howarth, 1903; Melmore, 1935, p. 31) as previously thought (Ford *et al*., 2008).

The visual difference between the two tills at Tunstall can potentially be explained by the local incorporation of rafts of the Sherwood Sandstone and /or Mercia Mudstone group (or rafts of till units rich in these materials). Intermixing of the two tills (e.g. **Figure 4d, e**) demonstrates that colour changes likely reflect subtle differences in till composition and sediment source rather than weathering. Similar red diamictons and sands interbedded with grey diamictons also occur within Devensian tills at Warren House Gill in Country Durham (Davies *et al*., 2012), indicating that this is a regional phenomenon. Whilst locally, this may enable the apparent sub-division of till units into Skipsea and Withernsea Till facies, at other sites to the north in Holderness (e.g. between Mappleton and Skipsea), facies of 'Withernsea Till' occur within the 'Skipsea Till' (Jonathan Lee, unpublished data). Principal Components Analysis also reveals subtle clast lithological variations within the till units demonstrating greater intra- rather than inter- till variability. Therefore, on the basis of clast lithological composition alone, it is difficult to discriminate between the two subglacial tills identified at Tunstall. In simple terms, there is not a consistent superpositional relationship between 'Skipsea Till' and 'Withernsea Till' facies in the Tunstall area and thus the lithostratigraphic scheme becomes unviable. This lithological analysis supports the findings from Boston *et al*. (2010), where geochemical analysis of LGM tills and glaciotectonites in east Yorkshire and Lincolnshire failed to precisely differentiate the Skipsea and Withernsea

Till types. This makes the application of the traditional nomenclature over a wider regional area tenuous.

Given that the stratigraphic succession at Tunstall cannot be assigned to the traditional bipartite sequence, we propose that inter- and intra-till variability relates to changes in subglacial debris provenance. Variations in debris provenance can be explained by both temporal and spatial changes in the availability of source materials implying that geological sources cycled through phases of active and non-entrainment. This entrainment could occur by melt and refreeze at the margins of the glacier prior to advance, by active shearing of overridden stony permafrost, from supraglacial sources, or by normal melt-freeze entrainment processes in temperate ice (Alley *et al*., 1997) whereby the glacier actively entrains basal material derived from the substrate by abrasion. To readily entrain debris into the basal layers of glacial ice, debris entrainment encompasses the detachment of frozen blocks of sediment from the subglacial substrate which is then folded and thrusted. The general entrainment mechanisms for basal debris transportation make these units rheologically distinct. It is suggested that this behaviour may relate to changes in subglacial conditions and behaviour. For example, the temporary burial (or exposure) of a specific source material and/or changes in the subglacial bed rheology which drive stick (erosion) and slip (non- or reduced entrainment) ice flow (Iverson, 2010; Iverson and Peterson, 2011; Phillips *et al*., 2018).

6.2 Genetic Model: the significance of fractures F1 – F3

Fractures F1-F3 are interpreted as being formed in response to unloading and shrinkage of the tills in response to the removal of overlying glacier ice, followed by consolidation and drying. F2 fractures are interpreted as unloading joints aligned perpendicular to the direction of unloading (vertical). The geometry of the F2 fracture implies that the fracture developed on a pre-existing, regionally-extensive plane of weakness such as a décollement surface.

646 The simplest interpretation is that this décollement surface originally formed due to the low-
647 angle glaciotectonic thrust emplacement of a layer of LFA 1 on top of LFA 1 (cf. Hiemstra
648 *et al*., 2007; Lee *et al*., 2013, 2017). The low-angle geometry of the décollement surface
649 implies that porewater pressures along the detachment were elevated (Phillips *et al*., 2008;
650 Lee *et al*., 2013, 2017). However, the sharpness of the fracture and absence of dewatering
651 structures (e.g. diffuse bedding, flame structures) suggests that a degree of consolidation and
652 dewatering of the lower unit of LFA 1 had occurred prior to thrusting indicating a possible
653 hiatus. Vertical fractures F1 and F3, produced during unloading and subsequent shrinkage,
654 are partitioned by sub-horizontal fracture F2. These fractures could have developed broadly
655 contemporaneously with F2 acting to partition stress, restricting the spatial development of
656 F1 and F3. Alternatively, F1 could predate F2, and F3 post-date F2. This would lend further
657 support to the interpretation that F2 is superimposed upon a relict thrust plane and that a
658 hiatus occurred during the accretion of LFA 1 resulting in partial consolidation and drying.
659 These characteristics, coupled with the emplacement of LFA 2 over LFA 1, are considered
660 to suggest a highly-dynamic temperate ice-marginal landsystem (cf. Evans and Twigg,
661 2002), characterised by multiple ice-marginal oscillations that resulted in the thrust-stacking
662 of multiple till blocks.

663 Till sequences produced by thrust-stacking typically create vertical, repetitive
664 sedimentological/lithological signatures observed frequently in exposures of glacial geology
665 elsewhere along the east coast of Britain (Boston *et al*., 2010; Evans and Thomson, 2010;
666 Lee *et al*., 2013, 2017). Although there are undoubtedly two till units (LFA 1 and LFA 2)
667 present at Tunstall, they have both been deposited by the NSL and reflect repeated ice-
668 marginal oscillations and till emplacement by thrust-stacking. We propose that the sequence
669 at Tunstall was generated by successive ice-margin oscillations, and are thereby suggestive
670 of active retreat (Boulton, 1996a, b; cf. Dove *et al*., 2018). Alternatively, as the substrate is

progressively buried by surficial deposits following each advance-retreat phase, the stacked sequence could be a function of reduced interaction of basal ice with the local lithologies (Boulton, 1996a, b; Kjær *et al*., 2006). In this case, the frequency of far-travelled lithological components of the till would increase with height and produce a similar lithological heterogeneity within samples, such as the results of this study.

6.3 A litho-tectonic event model for Tunstall

The fracture sets, lithological and sedimentological data from Tunstall enable an integrated litho-tectonic model for the site to be proposed (**Table 3**). In summary, the vertical and horizontal fractures provide a complementary record to the sedimentological and lithological analysis suggesting multiple phases of ice advance and retreat: (i) ice advance and accretion of the lower part of LFA 1; (ii) ice-marginal retreat, unloading, consolidation and shrinkage (formation of F1); (iii) brief hiatus; (iv) ice-marginal re-advance, thrust stacking of LFA 1 on top of LFA 1; (v) ice marginal retreat, unloading and horizontal fracturing (F2) developed along a pre-existing decollement surface; (vi) ice-marginal re-advance, emplacement of LFA 2; (vii) ice-marginal retreat, unloading, consolidation and shrinkage – formation of F3 fractures; (viii) sub-marginal deposition of glaciofluvial deposits LFA 3; (ix) non-glacial deposition of LFA 4 (x) coastal erosion and development of lateral release joints (formation of F4).

The application of lithostratigraphic principals to the Skipsea Till significantly under-represents the geological relevance of the 'unit' and specifically the number of ice-advances that formed the unit. This mirrors studies utilising glaciotectonic evidence elsewhere in eastern England, which records considerably much more dynamic phase of ice-marginal behaviour than shown by lithostratigraphic data alone (Lee and Phillips, 2008; Phillips *et al*., 2008; Lee *et al*., 2013; Phillips and Lee, 2013; Lee *et al*., 2017).

The presence of two distinctly different till units – the Skipsea and Withernsea tills, is also questioned based on lithological data. Instead the till units are interpreted as thrust-induced stacks of pre-existing till that accreted during cyclical oscillations of the ice margin (cf. Hiemstra *et al*., 2007; Lee *et al*., 2017) and up-ice variations in subglacial entrainment of bedrock lithologies. We therefore propose the term 'Skipsea till complex' to encompass the multiple thrust-stacked layers of till which cannot be classified lithostratigraphically.

7. CONCLUSIONS

The stratigraphic succession at Tunstall contains four lithofacies associations (LFA 1 - 4) and three primary fracture sets (F1 - F3) which collectively establish an event stratigraphy for the site encompassing the Late Devensian glaciation. The succession records two superimposed subglacial traction till units (LFA 1 and 2). Sub-horizontal fracture (F2) is interpreted as an unloading joint superimposed upon a regionally-extensive décollement surface formed during the thrust-stacking of a unit of LFA 1 on top of LFA 1. Vertical fractures F1 and F3 appear to relate to shrinkage and are tentatively interpreted to indicate two separate phases of unloading and shrinkage that occurred following ice-marginal retreat intra-LFA 1 and following the accretion of LFA 2. LFA 3 and 4 record the transition to non-glacial conditions.

Clast lithological data have also been used to reconstruct glacial transport pathways for the tills at Tunstall during the Late Devensian glaciation. The data provide evidence in support of deposition by a lobe of glacier ice (first sourced from southern and central Scotland), that flowed southwards down the present east coast of England (and offshore area of the southern North Sea) before reaching its final extent on the Holderness coast. The provenance of both tills therefore indicate an exclusively northern British origin. However,

statistical analysis of the clast lithological data demonstrates that there is greater intra-till lithological variability within the tills than between the till units. We suggest this lithological variability reflects temporal and spatial variability in the availability and entrainment of bedrock source materials along the ice flow path. Furthermore, the two subglacial tills at Tunstall cannot be differentiated lithostratigraphically, nor can they be directly correlated with the regional glacial lithostratigraphy along the east and northeast coast of Britain. This supports similar assertions made previously by Boston *et al*. (2010) based on geochemical analysis from the Holderness tills.

Collectively, this evidence demonstrates that caution is required when applying lithostratigraphic principals to till because these can underestimate the history of ice advance and dynamic ice-marginal behaviour. In the case of this study, we consider that variations in till lithological properties are not clear-cut between till units. Instead, the variability in till composition reflects the temporal and spatial patterns of up-ice source material entrainment plus the local erosional processes driven by thrust-stacking at an oscillating ice margin.

ACKNOWLEDGEMENTS

This research was undertaken whilst the lead author was completing an MSc in Quaternary Science at Royal Holloway University of London in 2015. Fieldwork was supported by the Quaternary Research Association (QRA) New Research Workers Award. Adrian Palmer is thanked for his help in the laboratory. Gastropod identification was done by Jenni Sherriff. Jonathan Carrivick commented on a draft of this manuscript. JRL publishes with the permission of the Executive Director of the British Geological Survey. Mark Bateman, Rodger Connell and Emrys Phillips are thanked for their discussion. We also thank an

743 anonymous reviewer and Clare Boston for providing constructive reviews on the
744 manuscript.
745

REFERENCES

Andrews, J. E., Pedley, M., and Dennis, P. F. 2000. Palaeoenvironmental records in Holocene Spanish tufas: a stable isotope approach in search of reliable climatic archives. *Sedimentology*, *47*(5), 961-978

Bamber, J. L., Riva, R. E., Vermeersen, B. L., and LeBrocq, A. M. 2009. Reassessment of the potential sea-level rise from a collapse of the West Antarctic Ice Sheet. *Science*, *324*(5929), 901-903

Bateman, M. D., Buckland, P. C., Whyte, M. A., Ashurst, R. A., Boulter, C., and Panagiotakopulu, E. V. A. 2011. Re-evaluation of the Last Glacial Maximum typesite at Dimlington, UK. *Boreas*, *40*(4), 573-584

Bateman, M. D., Evans, D. J. A., Buckland, P. C., Connell, E. R., Friend, R. J., Hartmann, D., Moxon, H., Fairburn, W. A., Panagiotakopulu, E., and Ashurst, R. A. 2015. Last glacial dynamics of the Vale of York and North Sea lobes of the British and Irish Ice Sheet. *Proceedings of the Geologists' Association*, *126*(6), 712-730

Bateman, M. D., Evans, D. J., Roberts, D. H., Medialdea, A., Ely, J., and Clark, C. D. 2017. The timing and consequences of the blockage of the Humber Gap by the last British− Irish Ice Sheet. *Boreas 47*, 41-61

Bell, F. G., and Forster, A. 1991. The geotechnical characteristics of the till deposits of Holderness. *Geological Society, London, Engineering Geology Special Publications*, *7*(1), 111-118

Benn, D. I. 1994. Fabric shape and the interpretation of sedimentary fabric data. *Journal of Sedimentary Research*, 64(4), 910-915

768 Bennett, M. R., Waller, R. I., Glasser, N. F., Hambrey, M. J., and Huddart, D. 1999.
769 Glacigenic clast fabrics: genetic fingerprint or wishful thinking? *Journal of*
770 *Quaternary Science, 14*(2), 125-135

771 Bird, E. ed., 2010. *Encyclopedia of the world's coastal landforms*. Springer Science and
772 Business Media

773 Bisat, W. S. 1939. Older and newer drift in East Yorkshire. In *Proceedings of the Yorkshire*
774 *Geological and Polytechnic Society, Geological Society of London, 24(3),* 137-151

775 Boston, C. M., Evans, D. J. A., and Ó Cofaigh, C. 2010. Styles of till deposition at the
776 margin of the Last Glacial Maximum North Sea lobe of the British–Irish Ice Sheet:
777 an assessment based on geochemical properties of glacigenic deposits in eastern
778 England. *Quaternary Science Reviews*, *29*(23), 3184-3211

779 Boulton, G. S. 1996a. The origin of till sequences by subglacial sediment deformation
780 beneath mid-latitude ice sheets. *Annals of Glaciology*, *22*(1), 75-84

781 Boulton, G. S. 1996b. Theory of glacial erosion, transport and deposition as a consequence
782 of subglacial sediment deformation. *Journal of Glaciology*, *42*(140), 43-62

783 Boulton, G.S., and Paul, M.A. 1976. The influence of genetic process on some
784 geotechnical properties of glacial tills. *Quarterly Journal of Engineering Geology*,
785 9, 159-194

786 Boulton, G. S., and Hindmarsh, R. C. A. 1987. Sediment deformation beneath glaciers:
787 rheology and geological consequences. *Journal of Geophysical Research: Solid*
788 *Earth*, *92*, 9059-9082

789 Bridgland, D. R. 1986. *Clast lithological analysis* (No. 3). Quaternary Research
790 Association

791 Busfield, M. E., Lee, J. R., Riding, J. B., Zalasiewicz, J., and Lee, S. V. 2015. Pleistocene
792 till provenance in east Yorkshire: reconstructing ice flow of the British North Sea
793 Lobe. *Proceedings of the Geologists' Association*, *126*(1), 86-99

794 Cameron, I. B., and Stephenson, D. 1985. *British regional geology: the Midland Valley of*
795 *Scotland* (No. 5). Hmso Books

796 Carr, S. J., Holmes, R. V. D., Van der Meer, J. J. M., and Rose, J. 2006. The Last Glacial
797 Maximum in the North Sea Basin: micromorphological evidence of extensive
798 glaciation. *Journal of Quaternary Science*, *21*(2), 131-153

799 Castedo, R., de la Vega-Panizo, R., Fernández-Hernández, M. and Paredes, C. 2015.
800 Measurement of historical cliff-top changes and estimation of future trends using
801 GIS data between Bridlington and Hornsea–Holderness Coast (UK).
802 *Geomorphology*, *230*, pp.146-160

803 Catt, J. A. 2007. The Pleistocene glaciations of eastern Yorkshire: a review. *Proceedings of*
804 *the Yorkshire Geological Society*, *56*(3), 177-207

805 Catt, J. A., and Digby, P. G. N. 1988. Boreholes in the Wolstonian Basement Till at
806 Easington, Holderness, July 1985. In *Proceedings of the Yorkshire Geological and*
807 *Polytechnic Society*, Geological Society of London, 47(1), 21-27

808 Catt, J. A., and Penny, L. F. 1966. The Pleistocene deposits of Holderness, East
809 Yorkshire. *Proceedings of the Yorkshire Geological Society*, *35*(3), 375-420

810 Cheshire, D. A. 1986. *The lithology and stratigraphy of the Anglian deposits of the Lea*
811 *basin* (Doctoral dissertation, Hatfield Polytechnic).

812 Clark, C. D., Hughes, A. L., Greenwood, S. L., Jordan, C., and Sejrup, H. P. 2012. Pattern
813 and timing of retreat of the last British-Irish Ice Sheet. *Quaternary Science*
814 *Reviews*, *44*, 112-146

Clark, C. D., Ely, J. C., Greenwood, S. L., Hughes, A. L. C., Meehan, R., Barr, I. D., Bateman, M. D., Bradwell, T., Doole, J., Evans, D. J. A., Jordan, C. J., Monteys, X., Pellicer, X. M., Sheehy, M., 2018. BRITICE Glacial Map, version 2: a map and GIS database of glacial landforms of the last British–Irish Ice Sheet. *Boreas, 47 (1)*, 11-18

Collinson, J. D. 1996. Alluvial Sediments. In, Reading, H. G. (ed). Sedimentary environments: processes, facies and stratigraphy.

Cossart, E., Braucher, R., Fort, M., Bourlès, D.L. and Carcaillet, J. 2008. Slope instability in relation to glacial debuttressing in alpine areas (Upper Durance catchment, southeastern France): Evidence from field data and 10Be cosmic ray exposure ages. *Geomorphology*, *95*(1-2), 3-26

Cotterill, C. J., Phillips, E., James, L., Forsberg, C. F., Tjelta, T. I., Carter, G., and Dove, D. 2017. The evolution of the Dogger Bank, North Sea: A complex history of terrestrial, glacial and marine environmental change. *Quaternary Science Reviews*, *171*, 136-153

Davies, B. J., Roberts, D. H., Ó Cofaigh, C., Bridgland, D. R., Riding, J. B., Phillips, E. R., and Teasdale, D. A. 2009. Interlobate ice-sheet dynamics during the Last Glacial Maximum at Whitburn Bay, County Durham, England. *Boreas*, *38*(3), 555-578

Davies, B. J., Roberts, D. H., Bridgland, D. R., Ó Cofaigh, C., and Riding, J. B. 2011. Provenance and depositional environments of Quaternary sediments from the western North Sea Basin. *Journal of Quaternary Science*, *26*(1), 59-75

Davies, B. J, Roberts, D. H, Bridgland, D. R, Ó Cofaigh, C, Riding, J. B, Demarchi, B, Penkman, K. E. H., and Pawley, S. M. 2012. Timing and depositional environments of a

838 Middle Pleistocene glaciation of northeast England: New evidence from Warren House Gill,
839 County Durham. *Quaternary Science Reviews, 44*, 180-212

840 Davies, B, Yorke, L, Bridgland, D and Roberts, D., (eds), 2013, *Quaternary of*
841 *Northumberland, Durham and Yorkshire*. Quaternary Research Association,
842 London, pp 208

843 Davies, B.J., Livingstone, S.J., Roberts, D.H., Evans, D.J.A., Gheorghiu, D.M. and Cofaigh,
844 C.Ó. 2019. Dynamic ice stream retreat in the central sector of the last British-Irish
845 Ice Sheet. *Quaternary Science Reviews*, *225*;

846 Davies, B.J., Livingstone, S.J., Roberts, D.H., Evans, D.J.A., Gheorghiu, D.M. and Cofaigh,
847 C.Ó., 2019. Dynamic ice stream retreat in the central sector of the last British-Irish
848 Ice Sheet. *Quaternary Science Reviews*, *225*

849 Davis, J. C. 1986: Statistics and Data Analysis in Geology. 656 pp. John Wiley & Sons

850 DeConto, R.M. and Pollard, D., 2016. Contribution of Antarctica to past and future sea-
851 level rise. *Nature*, *531*(7596), 591

852 Dehandschutter, B., Vandycke, S., Sintubin, M., Vandenberghe, N., and Wouters, L. 2005.
853 Brittle fractures and ductile shear bands in argillaceous sediments: inferences from
854 Oligocene Boom Clay (Belgium). *Journal of Structural Geology*, *27*, 1095-1112.

855 Dove, D., Evans, D. J., Lee, J. R., Roberts, D. H., Tappin, D. R., Mellett, C. L., Long, D.,
856 and Callard, S. L. 2017. Phased occupation and retreat of the last British–Irish Ice
857 Sheet in the southern North Sea; geomorphic and seismostratigraphic evidence of a
858 dynamic ice lobe. *Quaternary Science Reviews, 163*, 114-134

859 Dowdeswell, J. A., Ottesen, D., and Rise, L. 2006. Flow switching and large-scale
860 deposition by ice streams draining former ice sheets. *Geology*, *34*(4), 313-316

Edwards, C. A. 1981. ‘The tills of Filey Bay’, in Neale J. and Flenley, J. (Eds), The Quaternary in Britain, Pergamon Press, Oxford.

Edwards, C. A. 1987. ‘The Quaternary deposits in Filey Bay’, in Ellis, S. (Ed.), *East Yorkshire Filed Guide.* Quaternary Research Association, 15-21

Ely, J. C., Clark, C. D., Hindmarsh, R. C., Hughes, A. L., Greenwood, S. L., Bradley, S. L., Gasson, E., Gregoire, L., Gandy, N., Stokes, C. R, and Small, D. 2019. Recent progress on combining geomorphological and geochronological data with ice sheet modelling, demonstrated using the last British–Irish Ice Sheet. *Journal of Quaternary Science* 1-15

Emery, A. R., Hodgson, D. M., Barlow, N. L., Carrivick, J. L., Cotterill, C. J., Mellett, C. L., and Booth, A. D. 2019. Topographic and hydrodynamic controls on barrier retreat and preservation: An example from Dogger Bank, North Sea. *Marine Geology*, 105981

Evans, D. J. A. and Benn, D. I. 2004: A Practical Guide to the Study of Glacial Sediments. 206 pp. Arnold, London.

Evans, D. J. A., Bateman, M. D., Roberts, D. H., Medialdea, A., Hayes, L., Duller, G. A., and Clark, C. D. 2016. Glacial Lake Pickering: stratigraphy and chronology of a proglacial lake dammed by the North Sea Lobe of the British–Irish Ice Sheet. *Journal of Quaternary Science, 32(2),* 295-310

Evans, D. J. A., Lemmen, D. S. and Rea, B. R. 1999. Glacial landsystems of the southwest Laurentide Ice Sheet: modern Icelandic analogues. *Journal of Quaternary Science, 14*, 673–691

883 Evans, D. J. A., Owen, L. A. and Roberts, D. H. 1995. Stratigraphy and sedimentology of
884 Devensian (Dimlington Stadial) glacial deposits, East Yorkshire, England. *Journal*
885 *of Quaternary Science*, *10*, 241–265

886 Evans, D. J. A., Phillips, E. R., Hiemstra, J. F., and Auton, C. A. 2006. Subglacial till:
887 formation, sedimentary characteristics and classification. *Earth-Science*
888 *Reviews*, *78*(1), 115-176

889 Evans, D. J. A., and Thomson, S. A. 2010. Glacial sediments and landforms of Holderness,
890 eastern England: a glacial depositional model for the North Sea Lobe of the British–
891 Irish Ice Sheet. *Earth-Science Reviews*, *101*(3), 147-189

892 Evans, D.J.A., Twigg, D.R., 2002. The active temperate glacial landsystem: a model based
893 on Breiðamerkurjökull and Fjallsjökull, Iceland. *Quaternary Science Reviews*, 21,
894 2143-2177.

895 Evans, D. J. A,, Bateman, M. D., Roberts, D. H., Medialdea, A., Hayes, L., Duller, G. A.,
896 Fabel, D., and Clark, C. D. 2017. Glacial Lake Pickering: stratigraphy and
897 chronology of a proglacial lake dammed by the North Sea Lobe of the British–Irish
898 Ice Sheet. *Journal of Quaternary Science*, *32*(2), 295-310

899 Evans, D. J. A., Clark, C. D., and Mitchell, W. A. 2005. The last British Ice Sheet: A review
900 of the evidence utilised in the compilation of the Glacial Map of Britain. *Earth-*
901 *Science Reviews*, *70*(3), 253-312

902 Evans, D. J. A., Dinnage, M., and Roberts, D. H. 2018. Glacial geomorphology of
903 Teesdale, northern Pennines, England: Implications for upland styles of ice stream
904 operation and deglaciation in the British-Irish Ice Sheet. *Proceedings of the*
905 *Geologists' Association*, *129*(6), 697-735

906 Evans, D.J.A., Roberts, D.H., Bateman, M.D., Ely, J., Medialdea, A., Burke, M.J.,
907 Chiverrell, R.C., Clark, C.D., Fabel, D., 2019. A chronology for North Sea Lobe
908 advance and recession on the Lincolnshire and Norfolk coasts during MIS 2 and 6.
909 *Proceedings of the Geologists' Association*, 130, 523-540.

910 Evans, D.J.A., Thomson, S.A., Clark, C.D., 2001. Introduction to the Late Quaternary of
911 East Yorkshire and North Lincolnshire, in: Bateman, M.D., Buckland, P.C.,
912 Frederick, C.D., Whitehouse, N.J. (Eds.), The Quaternary of East Yorkshire and
913 North Lincolnshire. Field Guide. Quaternary Research Association, London, pp. 1-
914 12

915 Everest, J., Bradwell, T., and Golledge, N. 2005. Subglacial landforms of the tweed palaeo-
916 ice stream. *The Scottish Geographical Magazine*, *121*(2), 163-173

917 Eyles, N., Sladen, J. A., and Gilro, S. 1982. A depositional model for stratigraphic
918 complexes and facies superimposition in lodgement tills. *Boreas*, *11*(4), 317-333

919 Eyles, N., and McCabe, A. M. 1989. The Late Devensian (< 22,000 BP) Irish Sea Basin: the
920 sedimentary record of a collapsed ice sheet margin. *Quaternary Science*
921 *Reviews*, *8*(4), 307-351

922 Eyles, N., McCabe, A. M., and Bowen, D. Q. 1994. The stratigraphic and sedimentological
923 significance of Late Devensian ice sheet surging in Holderness, Yorkshire,
924 UK. *Quaternary Science Reviews*, *13*(8), 727-759

925 Fairburn, W. A., and Bateman, M. D. 2016. A new multi-stage recession model for
926 Proglacial Lake Humber during the retreat of the last British–Irish Ice
927 Sheet. *Boreas*, *45*(1), 133-151

928 Ford, J. R., Cooper, A., Price, S. J., Gibson, A., Pharaoh, T. C., and Kessler, H., 2008.
929 Geology of the Selby district: a brief explanation of the geological map Sheet 71
930 Selby. British Geological Survey, Keyworth Nottingham, HMSO

931 Gale, S., and Hoare, P. G. 2012. *Quaternary sediments: petrographic methods for the study*
932 *of unlithified rocks*. Blackburn Press

933 Gandy, N., Gregoire, L.J., Ely, J., Clark, C., Hodgson, D.M., Lee, V., Bradwell, T. and
934 Ivanovic, R.F. 2018. Marine ice sheet instability and ice shelf buttressing of the
935 Minch Ice Stream, northwest Scotland. *The Cryosphere*, *12*; 3635-3651

936 Gandy, N., Gregoire, L.J., Ely, J.C., Cornford, S.L., Clark, C.D. and Hodgson, D.M. 2019.
937 Exploring the ingredients required to successfully model the placement, generation,
938 and evolution of ice streams in the British-Irish Ice Sheet. *Quaternary Science*
939 *Reviews*, *223*;

940 Garnett, E. R., Gilmour, M. A., Rowe, P. J., Andrews, J. E., and Preece, R. C. 2004. 230
941 Th/234 U dating of Holocene tufas: possibilities and problems. *Quaternary Science*
942 *Reviews*, *23*(7), 947-958

943 Gaunt, G. 1975. The Devensian maximum ice limit in the Vale of York. Proceedings of the
944 Yorkshire Geological and Polytechnic Society, Geological Society of London

945 Genter, A., Duperret, A., Martinez, A., Mortimore, R.N. and Vila, J.L. 2004. Multiscale
946 fracture analysis along the French chalk coastline for investigating erosion by cliff
947 collapse. *Geological Society, London, Engineering Geology Special Publications*,
948 *20*(1), 57-74

949 Gibbard, P. L. 1985. *The Pleistocene History of the Middle Thames Valley*. Cambridge
950 University Press

951 Gibbard, P. L. 1986. Comparison of the clast lithological composition of gravels in the
952 Middle Thames using canonical variates analysis and principal components
953 analysis. *Clast Lithological Analysis. Technical Guide*, (3)

954 Greig, D. C., and Pringle, J. 1971. *British regional geology: the south of Scotland*. HMSO

955 Hambrey, M. J., and Glasser, N. F. 2012. Discriminating glacier thermal and dynamic
956 regimes in the sedimentary record. *Sedimentary Geology*, *251*, 1-33

957 Hart, J. K. 1997. The relationship between drumlins and other forms of subglacial
958 glaciotectonic deformation. *Quaternary Science Reviews*, *16*(1), 93-107

959 Hicock, S. R., and Fuller, E. A. 1995. Lobal interactions, rheologic superposition, and
960 implications for a Pleistocene ice stream on the continental shelf of British
961 Columbia. *Geomorphology*, *14*(2), 167-184

962 Hiemstra, J. F., Evans, D. J., and Ó Cofaigh, C. 2007. The role of glacitectonic rafting and
963 comminution in the production of subglacial tills: examples from southwest Ireland
964 and Antarctica. *Boreas*, *36*(4), 386-399

965 Hubbard, A., Bradwell, T., Golledge, N., Hall, A., Patton, H., Sugden, D., Cooper, R., and
966 Stoker, M. 2009. Dynamic cycles, ice streams and their impact on the extent,
967 chronology and deglaciation of the British–Irish ice sheet. *Quaternary Science*
968 *Reviews*, *28*(7), 758-776

969 Hubbard, B., and Glasser, N. F. 2005. *Field techniques in glaciology and glacial*
970 *geomorphology*. John Wiley & Sons

971 Hughes, A. L., Gyllencreutz, R., Lohne, Ø. S., Mangerud, J., and Svendsen, J. I. 2016. The
972 last Eurasian ice sheets–a chronological database and time-slice reconstruction,
973 DATED-1. *Boreas 45(1)*, 1-45

974 Iverson, N.R. 2010. Shear resistance and continuity of subglacial till: hydrology rules.
975 *Journal of Glaciology*, *56*(200), 1104-1114

976 Iverson, N.R. and Petersen, B.B. 2011. A new laboratory device for study of subglacial
977 processes: first results on ice–bed separation during sliding. *Journal of Glaciology*,
978 *57*(206), 1135-1146

979 Jones, J.M., Magraw, D., O'Mara, P.T., 1995. "Carboniferous and Westphalian coal
980 measures". In Johnson, G.A.L., 1995 (ed.), "Robson's Geology of northeast
981 England". *Transactions of the Natural History Society of Northumbria,* Volume 56,
982 Part 5, p. 267-282.

983 Kent, P., 1980. British regional Geology: Eastern England from the Tees to the Wash.
984 *Institute of Geological Sciences.* Natural Environment Research Council. HMSO,
985 London. Pp. 155

986 Kerney, M. P., Preece, R. C., and Turner, C. 1980. Molluscan and plant biostratigraphy of
987 some Late Devensian and Flandrian deposits in Kent. *Philosophical Transactions of*
988 *the Royal Society of London. Series B, Biological Sciences,* 1-43

989 Kjær, K. H., Larsen, E., van der Meer, J., Ingólfsson, Ó., Krüger, J., Benediktsson, Í. Ö.,
990 Knudsen, C. G., and Schomacker, A. 2006. Subglacial decoupling at the
991 sediment/bedrock interface: a new mechanism for rapid flowing ice. *Quaternary*
992 *Science Reviews*, *25*(21), 2704-2712

993 Kovach, W. L. 1995: Multivariate analysis. In Maddy, D. and Brew, J. S. (eds.): *Statistical*
994 *Modelling of Quaternary Science Data*, 1–38. Technical Guide 5, Quaternary
995 Research Association, Cambridge

996 Lee, J. R., Rose, J., Riding, J. B., Moorlock, B. S., and Hamblin, R. J. 2002. Testing the case
997 for a Middle Pleistocene Scandinavian glaciation in Eastern England: evidence for a

998 Scottish ice source for tills within the Corton Formation of East Anglia,
999 UK. *Boreas, 31*(4), 345-355

1000 Lee, J. R. 2003. *Early and Middle Pleistocene lithostratigraphy and palaeo-environments in*
1001 *northern East Anglia* (Doctoral dissertation, Royal Holloway, University of London)

1002 Lee, J. R., 2009. Patterns of preglacial sedimentation and glaciotectonic deformation within
1003 early Middle Pleistocene sediments at Sidestrand, north Norfolk, UK. Proceedings of
1004 the Geologists' Association 120, 34-48.

1005 Lee, J. R., and Phillips, E. R. 2008. Progressive soft sediment deformation within a
1006 subglacial shear zone—a hybrid mosaic–pervasive deformation model for Middle
1007 Pleistocene glaciotectonised sediments from eastern England. *Quaternary Science*
1008 *Reviews, 27*(13), 1350-1362

1009 Lee, J.R., Phillips, E., Booth, S.J., Rose, J., Jordan, H.M., Pawley, S.M., Warren, M.,
1010 Lawley, R.S., 2013. A polyphase glacitectonic model for ice-marginal retreat and
1011 terminal moraine development: the Middle Pleistocene British Ice Sheet, northern
1012 Norfolk, UK. Proceedings of the Geologists' Association 124, 753-777.

1013 Lee, J.R., Wakefield, O.J.W., Phillips, E., Hughes, L., 2015. Sedimentary and structural
1014 evolution of a relict subglacial to subaerial drainage system and its hydrogeological
1015 implications: an example from Anglesey, north Wales, UK. Quaternary Science
1016 Reviews 109, 88-110.

1017 Lee, J.R., Phillips, E., Rose, J., and Vaughan-Hirsch, D. 2017. The Middle Pleistocene
1018 glacial evolution of northern East Anglia, UK: a dynamic tectonostratigraphic-
1019 parasequence approach. *Journal of Quaternary Science, 32(2),* 231-260

1020 Livingstone, S. J., Evans, D. J., Ó Cofaigh, C., Davies, B. J., Merritt, J. W., Huddart, D.,
1021 Mitchell, W. A., Roberts, D. H., and Yorke, L. 2012. Glaciodynamics of the central

sector of the last British–Irish Ice Sheet in Northern England. *Earth-Science Reviews, 111*(1), 25-55

Livingstone, S.J., Roberts, D.H., Davies, B.J., Evans, D.J.A., Ó Cofaigh, C, and Gheorghiu, D.M. 2015. Late Devensian deglaciation of the Tyne Gap Palaeo-Ice Stream, northern England. *Journal of Quaternary Science, 30(8),* 790-804

Lovell, H., Livingstone, S. J., Boston, C. M., Booth, A. D., Storrar, R. D., and Barr, I. D. (2019). Complex kame belt morphology, stratigraphy and architecture. *Earth Surface Processes and Landforms*

Macklin, M. G. 1998. The Quaternary of the Eastern Yorkshire Dales: Field gudie; the Holocene alluvial record. Quaternary Research association

Madgett, P. A. 1975. Re-interpretation of Devensian Till stratigraphy of eastern England. *Nature*, *253*(5487), 105

Madgett, P. A., and Catt, J. A. 1978. Petrography, stratigraphy and weathering of Late Pleistocene tills in East Yorkshire, Lincolnshire and north Norfolk. In *Proceedings of the Yorkshire Geological and Polytechnic Society 42(1),* 55-108. Geological Society of London

Maizels, J. 1995. Sediments and landforms of modern proglacial ter- restrial environments. In Menzies, J. (ed.): *Modern Glacial Environments: Processes, Dynamics and Sediments*, 365–416. Butterworth-Heinemann, Oxford

Maltman, A.J., 1994. *The Geological Deformation of Sediments*. Chapman and Hall, London.

McMillan, A. A., and Merritt, J. W. 2012. A new Quaternary and Neogene lithostratigraphical framework for Great Britain and the Isle of Man. *Proceedings of the Geologists' Association*, *123*(5), 679-691

Merritt, J.W., Connell, E.R. and Hall, A.M. 2017. Middle to Late Devensian glaciation of north-east Scotland: implications for the north-eastern quadrant of the last British–Irish ice sheet. *Journal of Quaternary Science*, *32*(2), 276-294

Mertens, J., Vandenberghe, N., Wouters, L. and Sintubin, M. 2003. The origin and development of joints in the Boom Clay Formation (Rupelian) in Belgium. In: Van Rensbergen, P., Hillis, R.R., Maltman, A.J. and Chorley, C.K. (Eds.)., *Subsurface Sediment Mobilization*. Geological Society Special Publications 217, London, pp. 311-323.

Miall, A. D. 1977. Lithofacies types and vertical profile models in braided river deposits: a summary. *Earth Science Reviews*, *13*, 1-62

Pawley, S. M., Bailey, R. M., Rose, J., Moorlock, B. S., Hamblin, R. J., Booth, S. J., and Lee, J. R. 2008. Age limits on Middle Pleistocene glacial sediments from OSL dating, north Norfolk, UK. *Quaternary Science Reviews*, *27*(13), 1363-1377

Penny, L.F., Coope, G.R. and Catt, J.A. 1969. Age and insect fauna of the Dimlington Silts, East Yorkshire. *Nature*, *224*(5214), 65

Phillips, E., Cotterill, C., Johnson, K., Crombie, K., James, L., Carr, S., and Ruiter, A. 2018. Large-scale glacitectonic deformation in response to active ice sheet retreat across Dogger Bank (southern central North Sea) during the Last Glacial Maximum. *Quaternary Science Reviews*, *179*, 24-47

Piotrowski, J. A., and Kraus, A. M. 1997. Response of sediment to ice-sheet loading in northwestern Germany: effective stresses and glacier-bed stability. *Journal of Glaciology*, *43*(145), 489-502

1069 Piotrowski, J. A., and Tulaczyk, S. 1999. Subglacial conditions under the last ice sheet in
1070 northwest Germany: ice-bed separation and enhanced basal sliding?. *Quaternary*
1071 *Science Reviews*, *18*(6), 737-751
1072 Piotrowski, J. A., Larsen, N. K., and Junge, F. W. 2004. Reflections on soft subglacial beds
1073 as a mosaic of deforming and stable spots. *Quaternary Science Reviews*, *23*(9), 993-
1074 1000
1075 Radge, G. W. 1939. The glaciation of north Cleveland. In *Proceedings of the Yorkshire*
1076 *Geological and Polytechnic Society* 24(3), 180-205. Geological Society of London
1077 Reid, C. 1885. *The geology of Holderness, and the adjoining parts of Yorkshire and*
1078 *Lincolnshire* (Vol. 47). HM Stationery Office.
1079 Reimann, C., Filzmoser, P., Garrett, R. G., and Dutter, R. 2008. Statistical data analysis
1080 explained. *Applied environmental statistics with R. England: Wiley & Sons Ltd*
1081 Richards, A. E. 1998. Re-evaluation of the Middle Pleistocene stratigraphy of
1082 Herefordshire, England. *Journal of Quaternary Science*, *13*(2), 115-136
1083 Roberts, D. H., and Hart, J. K. 2005. The deforming bed characteristics of a stratified till
1084 assemblage in north East Anglia, UK: investigating controls on sediment rheology
1085 and strain signatures. *Quaternary Science Reviews*, *24*(1), 123-140
1086 Roberts, D. H., Evans, D. J. A., Lodwick, J. and Cox, N. J. 2013. The subglacial and ice-
1087 marginal signature of the North Sea Lobe of the British-Irish Ice Sheet during the
1088 Last Glacial Maximumat Upgang, North Yorkshire, UK. *Proceedings of the*
1089 *Geologists'Association, 124*, 503–519
1090 Roberts, D. H., Evans, D. J., Callard, S. L., Clark, C. D., Bateman, M. D., Medialdea, A.,
1091 Dove, D., Coterill, C. J., Saher, M., Ó Cofaigh, C., Chiverrell, R. C. Moreton, S. G.,
1092 Fabel., D., and Bradwell. T. 2018. Ice marginal dynamics of the last British-Irish Ice

1093 Sheet in the southern North Sea: Ice limits, timing and the influence of the Dogger
1094 Bank. *Quaternary Science Reviews, 198*, 181-207

1095 Roberts, D. H., Grimoldi, E., Callard, L., Evans, D. J., Clark, C. D., Stewart, H. A., and
1096 Bateman, M. D. 2019. The mixed-bed glacial landform imprint of the North Sea
1097 Lobe in the western North Sea. *Earth Surface Processes and Landforms, 44*(6),
1098 1233-1258

1099 Robson, D.A., 1976. "A guide to the geology of the Cheviot Hills". *Transactions of the*
1100 *Natural History Society of Northumbria,* 43(1), pp. 23

1101 Rose, J. 1985. The Dimlington Stadial/Dimlington Chronozone: a proposal for naming the
1102 main glacial episode of the Late Devensian in Britain. *Boreas, 14*(3), 225-230

1103 Small, D., Clark, C.D., Chiverrell, R.C., Smedley, R.K., Bateman, M.D., Duller, G.A., Ely,
1104 J.C., Fabel, D., Medialdea, A. and Moreton, S.G. 2017. Devising quality assurance
1105 procedures for assessment of legacy geochronological data relating to deglaciation of
1106 the last British-Irish Ice Sheet. *Earth-Science Reviews, 164*; 232-250

1107 Scourse, J.D., Ward, S.L., Wainwright, A., Bradley, S.L. and Uehara, K. 2018. The role of
1108 megatides and relative sea level in controlling the deglaciation of the British–Irish
1109 and Fennoscandian ice sheets. *Journal of Quaternary Science, 33*(2); 139-149

1110 Scheib, A. J., Lee, J. R., Breward, N., and Riding, J. B. 2011. Reconstructing flow paths of
1111 the Middle Pleistocene British Ice Sheet in central-eastern England: the application
1112 of regional soil geochemical data. *Proceedings of the Geologists'*
1113 *Association, 122*(3), 432-444

1114 Scourse, J. D., Haapaniemi, A. I., Colmenero-Hidalgo, E., Peck, V. L., Hall, I. R., Austin,
1115 W. E., Knutz, P. C., and Zahn, R. 2009. Growth, dynamics and deglaciation of the

last British–Irish ice sheet: the deep-sea ice-rafted detritus record. *Quaternary Science Reviews*, *28*(27), 3066-3084

Smith, D.B., 1995. "Permian and Triassic". In Johnson, G.A.L., 1995 (ed.), "Robson's Geology of northeast England". *Transactions of the Natural History Society of Northumbria,* Volume 56, Part 5, p. 283-296

Stokes, C. R., Tarasov, L., Blomdin, R., Cronin, T. M., Fisher, T. G., Gyllencreutz, R., and Jakobsson, M. 2015. On the reconstruction of palaeo-ice sheets: recent advances and future challenges. *Quaternary Science Reviews*, *125*, 15-49

Stone, P, Millward, D, Young, B, Merritt, J. W., Clarke, S.M., McCormac, M., and Lawrence, D. J. D. 2010. British Regional Geology: Northern England (Firth edition). Keyworth, Nottingham: British Geological Survey, HMSO

Stow, D. A. 2005. *Sedimentary rocks in the Field: a colour guide*. Gulf Professional Publishing

Stroeven, A. P., Hättestrand, C., Kleman, J., Heyman, J., Fabel, D., Fredin, O., and Caffee, M. W. 2016. Deglaciation of fennoscandia. *Quaternary Science Reviews*, *147*, 91-121

Taylor, B. J., and Eastwood, T. 1971. *Northern England* (Vol. 7). HM Stationery Office.

Toghill, P. 2011. *The geology of Britain: an introduction*. Wiltshire, UK, Swanhill Press

Trewin, N. H. 2002. *The Geology of Scotland.* Fourth Edition. London, The Geological Society of London, pp. 576

van der Wateren, F. M. 1995. Structural geology and sedimentology of push moraines: processes of soft sediment deformation in a glacial environment and the distribution of glaciotectonic styles, *Mededelingen Rijks Geologische Dienst 54*

1139 Walder, J. S., and Fowler, A. 1994. Channelized subglacial drainage over a deformable
1140 bed. *Journal of Glaciology*, *40*(134), 3-15

1141 Walden, J. S. 2004. Particle Lithology (or mineral and geochemical analysis). *A practical*
1142 *guide to the study of glacial sediments*. In D. J. A. Evans and D. I. Benn. London,
1143 Arnold, 145-180

1144 Wood, S. V., and Rome, J. L. 1868. On the glacial and postglacial structure of Lincolnshire
1145 and south-east Yorkshire. *Quarterly Journal of the Geological Society*, *24*(1-2), 146-
1146 184

1147 **FIGURE CAPTIONS**

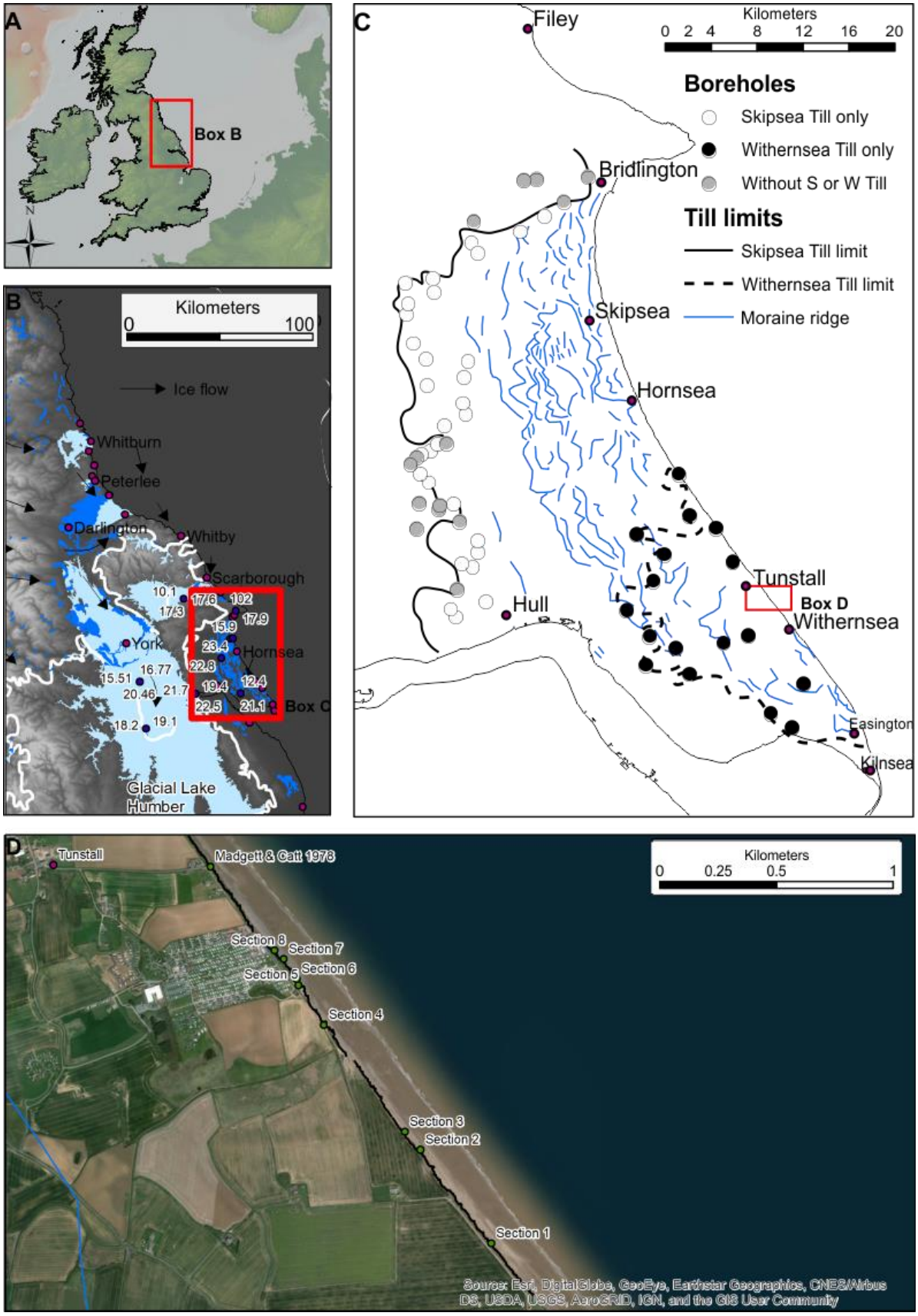

Figure 1. A. Great Britain and study area highlighted. **B.** The Yorkshire and Durham coastline, with places named in the text. **C.** Study area, showing limits of Skipsea and Withernsea Tills (from Evans and Thomson, 2010). Published ages and geomorphology

from Clark *et al*. (2018); Bateman *et al*. (2015; 2017); Evans *et al*. (2016). **D.** Detail of study area, showing location of section logs. Imagery from ArcMap Basemap

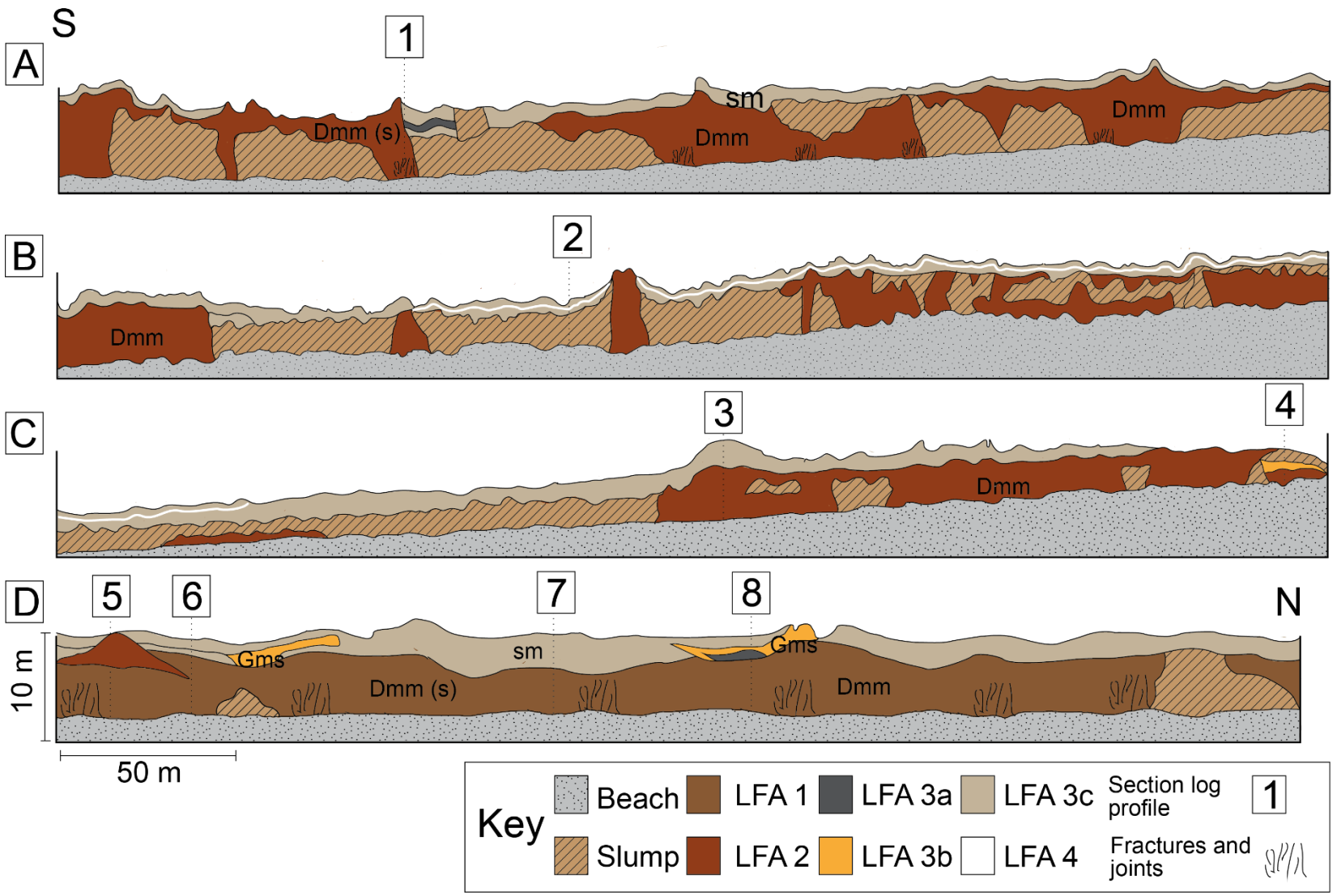

1156

1157 **Figure 2.** Facies architecture with clast fabric and straie orientation at Tunstall

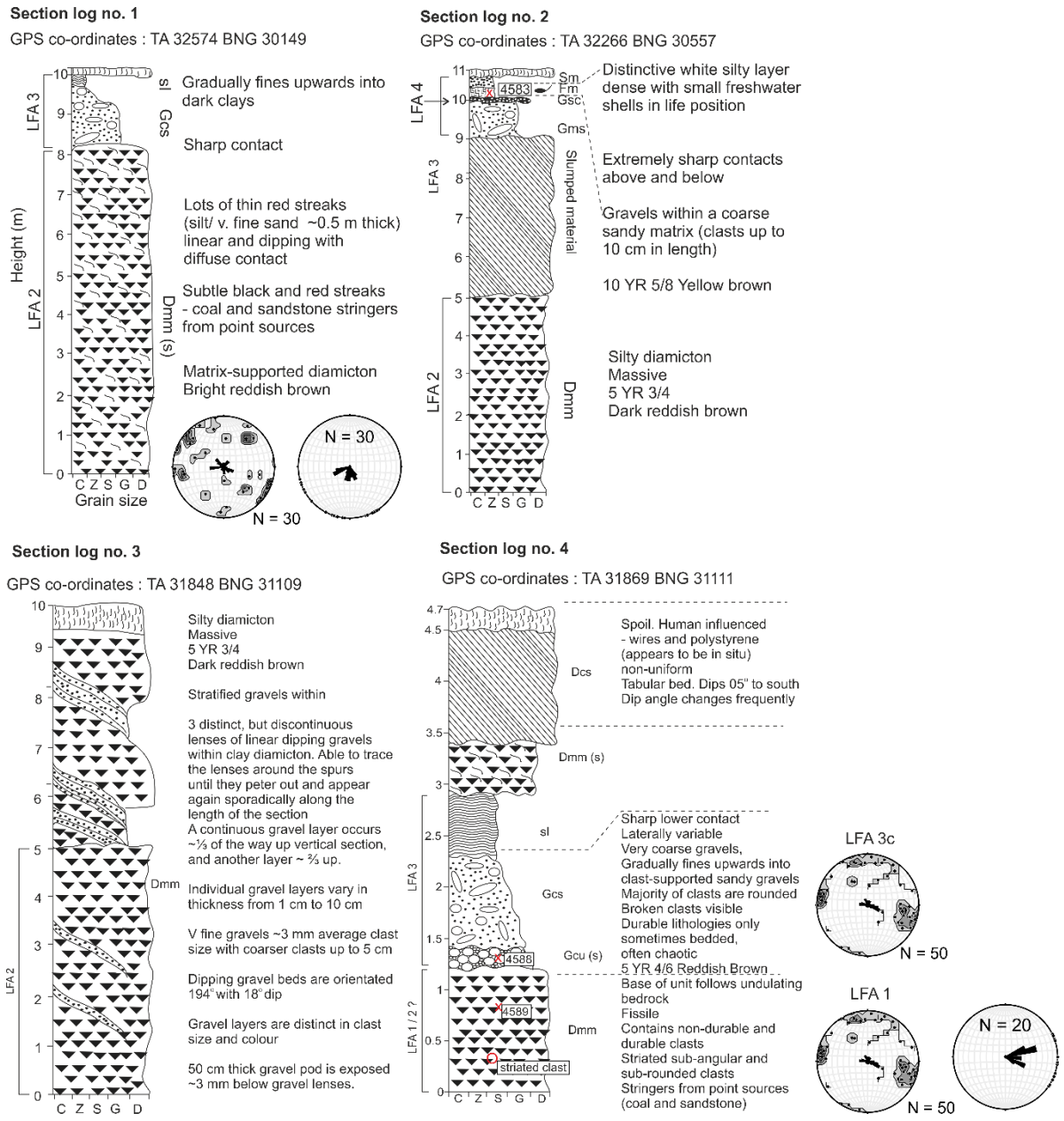

Figure 3a. Section logs 1 – 4 (see Figure 2 for log locations). Note differences in vertical scale

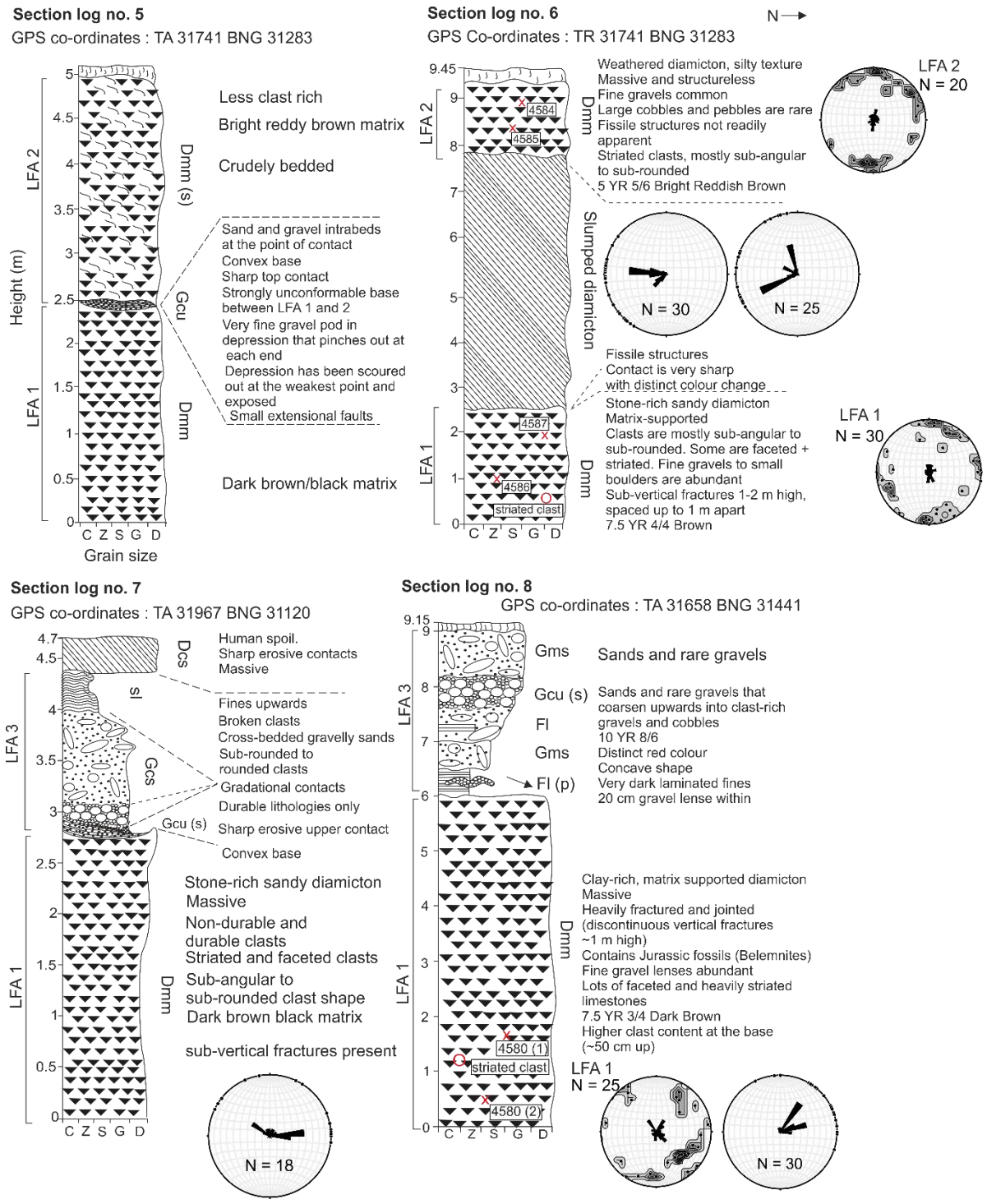

1161

1162 **Figure 3b.** Section logs 5 – 8 (see Figure 2 for log locations). Note differences in vertical

1163 scale

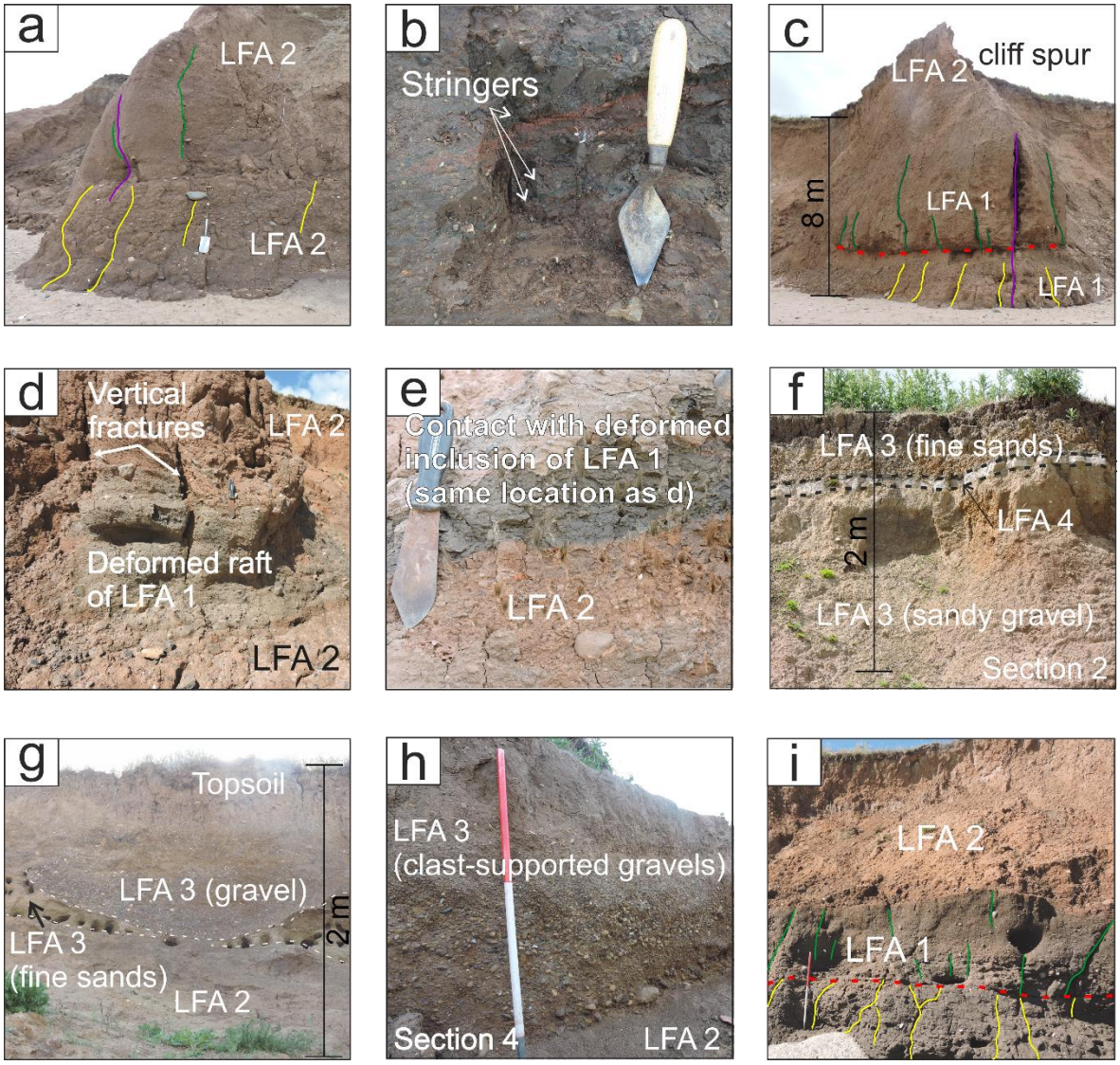

Figure 4. Representative photographs of key features at Tunstall including fracture sets F1 (yellow), F2 (red), F3 (green) and F4 (purple). **a.** LFA 1 and LFA 2 in superposition showing fracture sets **b.** Stringers of red and black diamicton up to 10 cm thick in LFA 1 **c.** Fracture sets F1, F2 and F3 in LFA 1 **d.** Raft of LFA 1 in LFA 2 **e.** Contact between LFA 2 and the deformed inclusion of LFA 1 **f.** Nature of LFA 4 **g.** Channel structure **h.** Cast-supported gravels in LFA 3 **i.** LFA 1 and 2 in superposition, showing F1 and F2 fracture sets

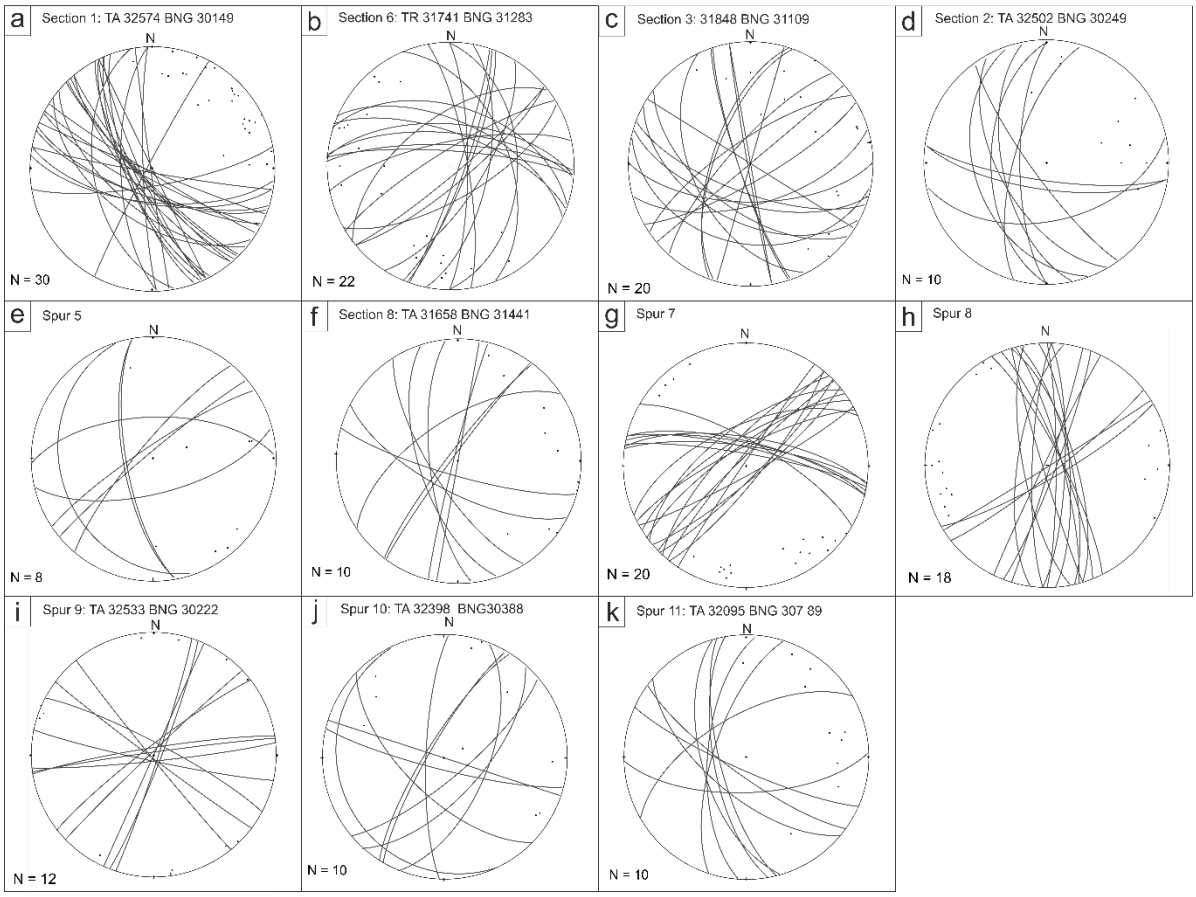

1171

1172 **Figure 5.** Fracture measurements (dip angle and dip azimuth) plotted as poles to planes and

1173 great circles on stereographic projections.

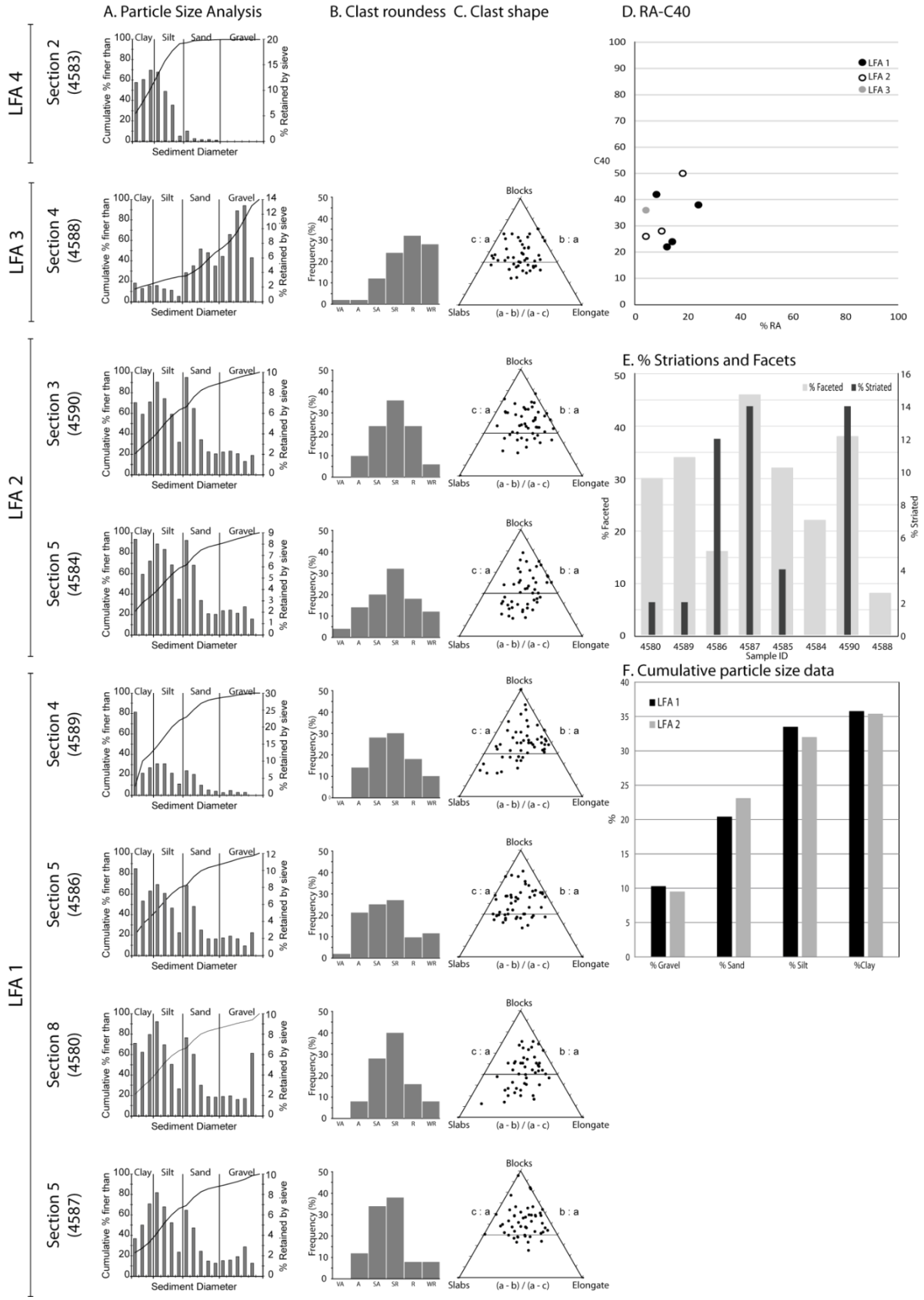

Figure 6. A. Particle size distribution for each sample. **B.** Clast roundness for gravel fraction. **C.** Clast shape for gravel fraction. **D.** RA-C40 graph. **E.** Percentage of striated and

faceted stones within the gravel fraction. **F.** Total percentages of clay, silt, sand and gravel in each lithofacies.

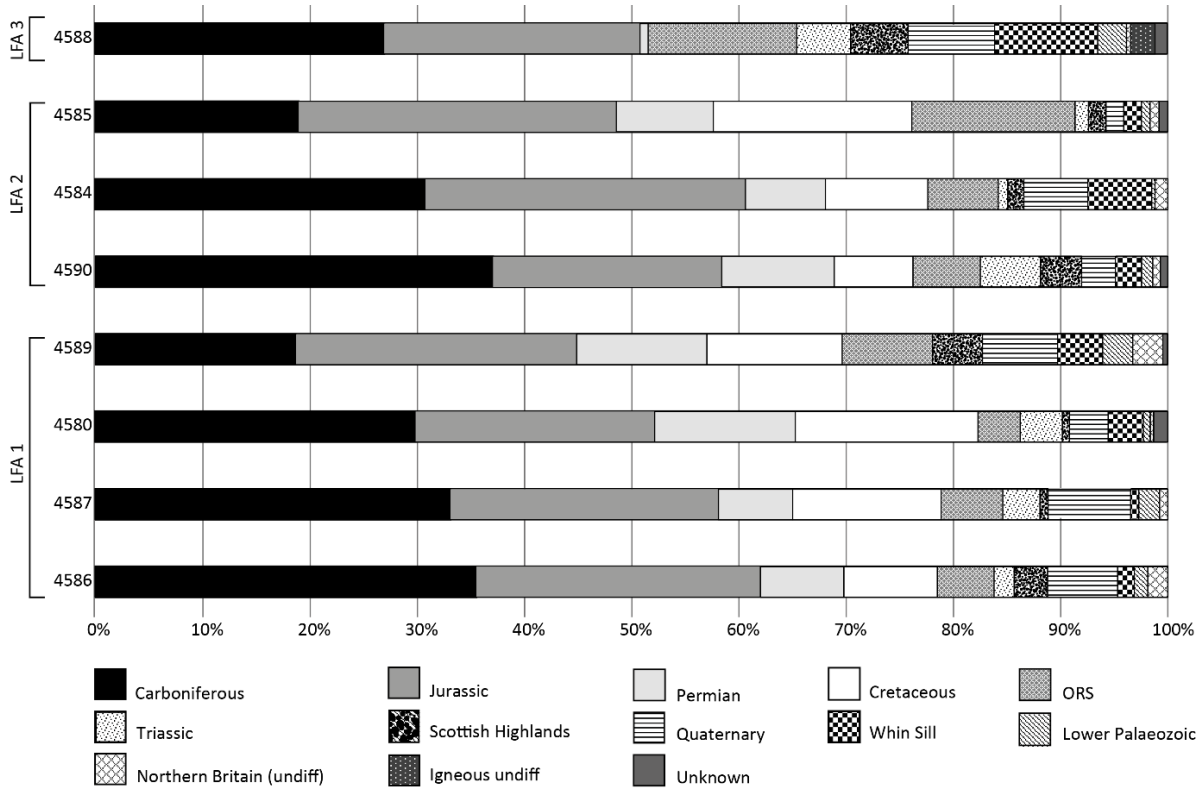

Figure 7. Clast lithological analysis for each sample

Figure 8. Representative photographs of key erratic lithologies in each sample **a.** Greywacke (LFA 2) **b.** Whin Sill Dolerite (LFA 2) **c.** Old Red Sandstone (LFA 1) **d.** Andesitic porphyry (LFA 2) **e.** Sherwood Sandstone (LFA 1) **f.** Magnesian Limestone (LFA 1) **g.** K-feldspar rich Granite (LFA 2) **h.** Rhyolite (LFA 3) **i.** Carboniferous Limestone (LFA 1) **j.** K-feldspar <Quartz Granodiorite (LFA 1) **k**. Cheviot Granite (LFA 3) **l.** Quartzite (LFA 1).

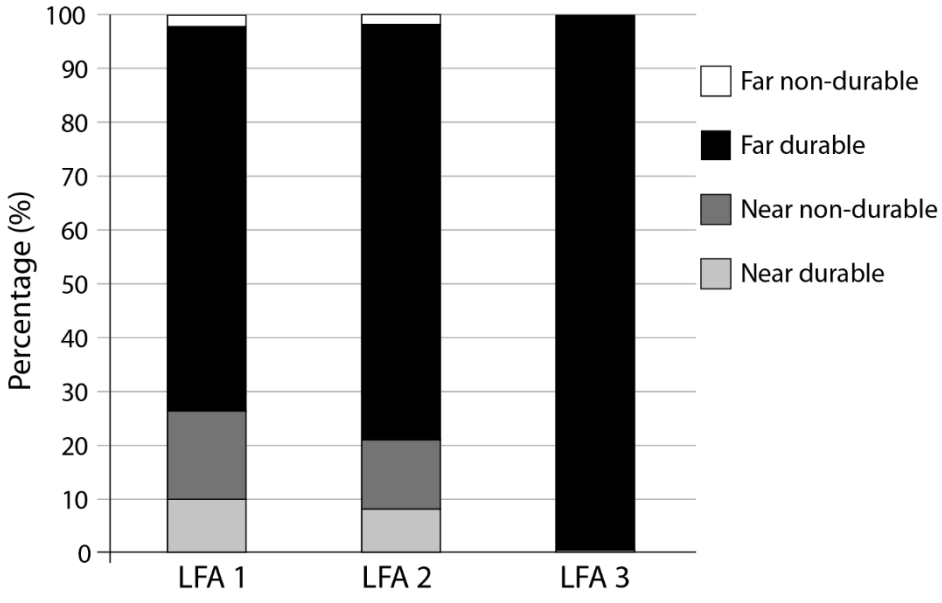

Figure 9. Durability of far travelled and local clasts in each lithofacies

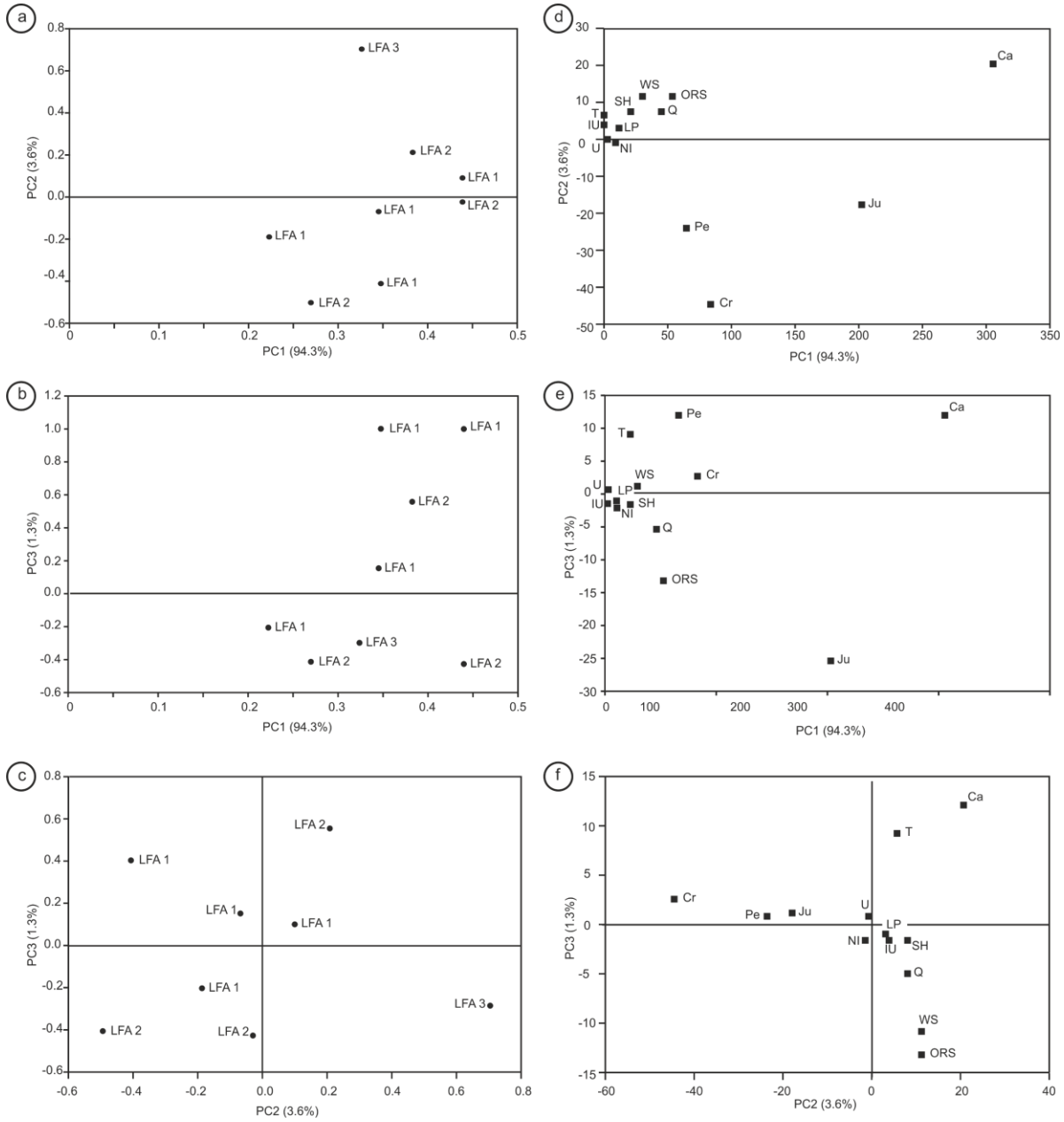

Figure 10. Plotting of processed PCA data. **a.** Principal component scores PC 1 and PC 2 **b.** Principal component scores PC 1 and PC 3 **c.** Principal component scores PC 2 and PC 3 **d.** Principal Component coefficients displaying lithological relationships between PC1 and PC2 **e.** Principal Component coefficients displaying lithological relationships between PC1 and PC3 **f.** Principal Component coefficients displaying lithological relationships between PC2 and PC3

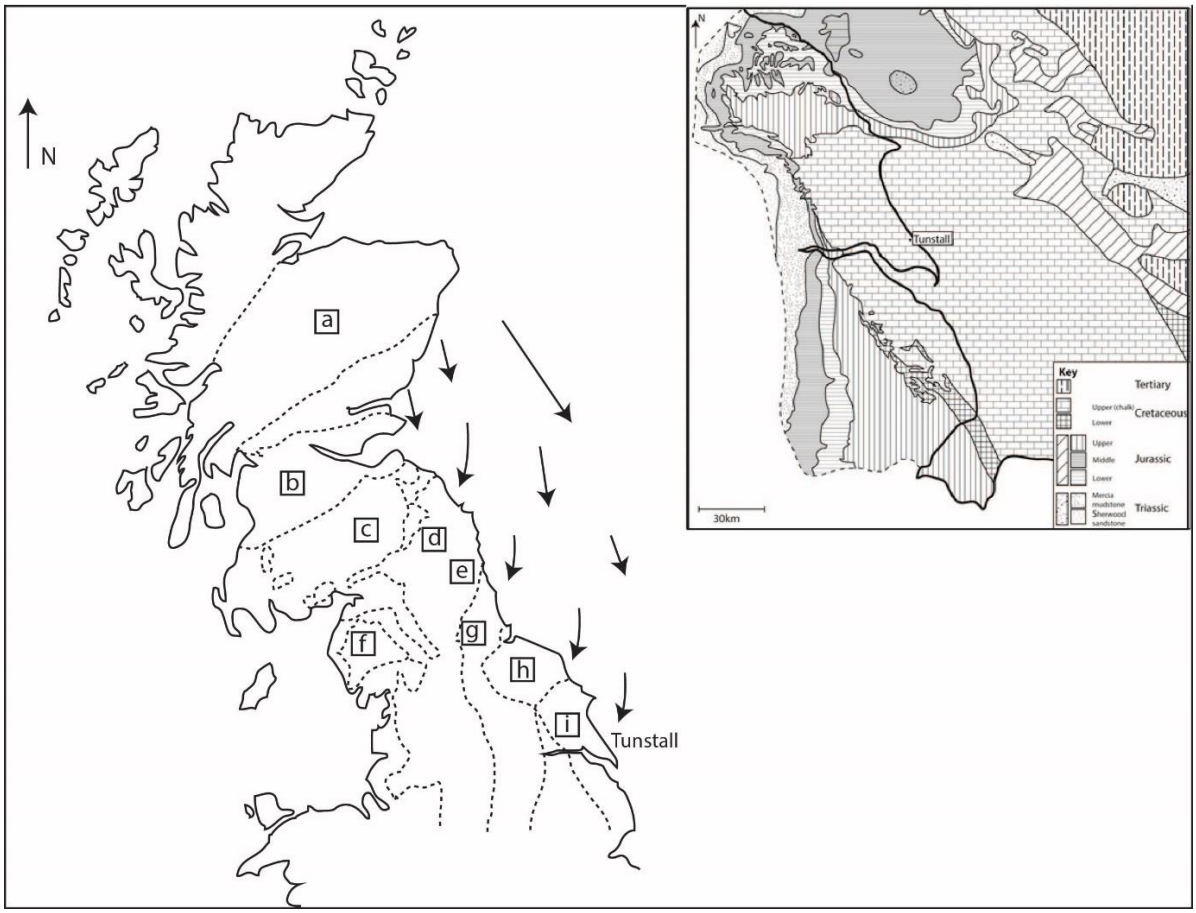

Figure 11. Revised iceflow pathways inferred from the simplified bedrock geology map of Northern Britain with outcrop occurances of the lithostratigraphical group .a. Grampian Highlands b. Midland Valley c. southern uplands d. Cheviot volcanic complex e. Northumberland f. Lake District volcanic complex g. County Durham h. Cleveland basin i. Yorkshire basin Insert – Detailed map of the solid geology from the Tees estuary to The Wash (adapted from Kent and Gaunt, 1980; Busfield *et al*., 2015).

TABLE CAPTIONS

	LFA 1	LFA 2	LFA 3	LFA 4
% Gravel	10.29	9.5	47.07	0.00
% Sand	20.41	23.1	27.74	3.22
% Silt	33.47	32	8.44	45.29
% Clay	35.78	35.4	16.75	51.49

Table 1. Particle size analysis for each lithofacies at Tunstall

1208

	Clast Lithology	LFA 1	LFA 2	LFA 3
Total (n)		**893**	**847**	**260**
Carboniferous	Arkose sandstone	2.46	4.57	0.00
	Carboniferous sandstone	13.66	18.44	26.54
	Carboniferous Chert	0.00	0.16	0.00
	Carboniferous Mudstone	0.00	0.16	0.00
	Carboniferous Limestone	9.52	7.38	0.00
	Coal	2.13	1.44	0.00
	Limestone undiff	3.81	0.64	0.00
	Basaltic Porphyry	0.56	0.96	0.38
	Carboniferous Porphyry	0.45	0.00	0.00
Permian	Sherwood Sandstone	2.69	3.05	0.77
	Magnesian Limestone	6.61	5.77	0.00
Triassic	Mercia Mudstone	3.02	3.05	0.00
	Red Siltstone	0.00	0.00	5.00
Jurassic	Jurassic Sandstone	6.16	7.54	3.08
	Yellow Sandstone	1.34	1.28	5.38
	Quartzitic Sandstone	1.12	0.96	0.00
	Siltstone undiff	4.03	6.26	8.46
	Yellow Siltstone	0.22	0.16	0.00
	Jurassic Mudstone	11.65	6.98	6.54
	Ironstone	0.00	0.80	0.38
	Jurassic Limestone	0.56	1.76	0.00
	Oolitic Limestone	0.00	0.16	0.00
Cretaceous	Cretaceous Chert	0.00	0.16	0.00
	Chert undiff	2.58	1.92	0.00
	Chalk	10.41	6.58	0.00
	Flint	0.22	0.32	1.54
Quaternary	Silcrete	0.00	0.16	0.00
	Brown Quartzite/ Vein Quartz	3.25	2.41	4.23
	Red Quartzite/ Vein Quartz	0.56	0.48	0.00
	White Quartzite/Vein Quartz	1.79	1.28	2.31
Lower Palaeozoic	Greywacke	1.23	0.48	2.69
Northern Britain	Gabbro	0.00	0.32	0.38
	Basalt	1.01	0.64	0.00
Whin Sill	Whin Sill Dolerite	1.90	4.33	9.62
Old Red Sandstone	Old Red Sandstone	2.91	2.25	6.15
	Old Red Sandstone porphyry	0.34	0.48	0.00
Scottish Highlands	Diorite	0.78	0.32	1.92
	Grano-diorite	0.22	0.16	0.00
	Micro-granite	0.00	1.12	3.08
	Granite	0.00	0.00	0.38
	Schist	0.45	0.48	0.00
	Phyllite	0.22	0.32	0.00
	Gneiss	0.00	0.08	0.00
Igneous	Igneous undiff	0.00	0.00	2.31
	Rhyolite	0.45	1.12	1.15
	Andesite	0.56	0.96	1.54
	Felsite	0.00	0.32	0.00
	Andesitic Porphyry	0.45	0.64	1.54
	Rhyolitic Porphyry	0.22	0.80	3.46
Unknown		0.45	0.32	1.15

1209 **Table 2.** Clast lithological data, showing percentages of clasts in each lithofacies

1210

Event/Stage	Description	Interpretation	Implication
I	Massive, matrix-supported diamicton	Deposition of subglacial traction till (LFA 1; lower Skipsea Till)	Initial advance from NSL
II	Sub-vertical fractures (upwards to F2)	Unloading and shrinkage; development of F1 fractures	Sub-aerial exposure of ice-marginal retreat or thinning
	Hiatus (Short)		
IV	Massive-matrix-supported diamicton	Thrust-stacking of LFA 1 (derived from nearby but up-ice) ontop of LFA 1 (decollement surface eventually became F2)	Re-advance of NSL
V	Sub-horizontal fracturing along pre-exiting plane of weakness (décollement developed in stage iv)	Unloading and development of F2 fractures	Retreat of the NSL
VI	Massive, matrix-supported diamicton	Subglacial emplacement of LFA 2	Re-advance of NSL
VII	Sub-vertical fractures (upwards from F2)	Unloading and shrinkage; development of F3 fractures	Subaerial exposure of ice-marginal retreat or thinning
VIII	Sands and gravels	Deposition of LFA 3; proximal glaciofluvial outwash	Retreat following advance but no overriding of site; final stages of deglaciation
IX	White organic silt	Deposition of LFA 4 (Tufa)	Spring-fed pool under temperate icefree conditions

	X	Sub-vertical fractures (F4)	Lateral release joints	Coastal erosion

Table 3. Summary of litho-tectonic event stratigraphy described from the base (oldest) to the top (youngest) in superpositional order

1213 **SUPPLEMENTARY INFORMATION**

Code	Description
	Diamictons
Dmm	Matrix-supported, massive
Dcs	Clast-supported, massive
---(s)	Stratified
	Gravels
Gms	Matrix-supported, massive
Gcs	Clast-supported
Gcu	Upwards coarsening gravels (inverse grading)
---(s)	Stratified
	Sands
Sm	Massive
Sl	Horizontal and draped lamination
	Silts and Clays
Fm	Massive
Fl	Fine lamination (minor sand and very small

	ripples
---*(p)*	Intraclast or lens

SUPPLEMENTARY Table A1. Lithofacies codes used in this study (and those in **Figure 3a**, **b**), adapted from Benn and Evans (1998)